47
7/1.2/84
(1) I-15850

ornl

ORNL/TM-8665
ORNL/TM--8665
TI84 027502

OAK RIDGE NATIONAL LABORATORY

MARTIN MARIETTA

The Rate of Pu(IV) Polymer Formation in Nitric Acid Solutions. A Parametric Study

L. M. Toth
M. M. Osborne

CONSOLIDATED FUEL REPROCESSING PROGRAM C F ORNL R P

OPERATED BY
MARTIN MARIETTA ENERGY SYSTEMS, INC.
FOR THE UNITED STATES
DEPARTMENT OF ENERGY

Printed in the United States of America. Available from
the U.S. Department of Energy
Technical Information Center
P.O. Box 62, Oak Ridge, Tennessee 37830

DISCLAIMER

ORNL/TM--8665

TI84 027502

ORNL/TM-8665
Dist. Category UC-86T
(Applied)

Consolidated Fuel Reprocessing Program

THE RATE OF Pu(IV) POLYMER FORMATION IN NITRIC ACID SOLUTIONS. A PARAMETRIC STUDY

L. M. Toth
M. M. Osborne

Chemical Technology Division

Date of Issue — July 1984

Prepared by the
OAK RIDGE NATIONAL LABORATORY
Oak Ridge, Tennessee 37831
operated by
MARTIN MARIETTA ENERGY SYSTEMS, INC.
for the
U.S. DEPARTMENT OF ENERGY
Under Contract No. DE-AC05-84OR21400

THE RATE OF Pu(IV) POLYMER FORMATION IN NITRIC ACID SOLUTIONS. A PARAMETRIC STUDY

L. M. Toth
M. M. Osborne

ABSTRACT

The kinetics of Pu(IV) polymer formation has been examined with the intent of developing a simple mathematical equation that would predict the appearance of polymer. The fundamental polymerization rate has been found to be dependent on $[Pu(IV)]^{1.2}$ and $[HNO_3]^{-6}_{real}$. The activation energy for polymer formation is temperature dependent, varying from 66.9 kJ/mol (16 kcal/mol) at 25°C to 150.5 kJ/mol (36 kcal/mol) at 105°C. These relationships have guided the development of an empirical model that gives "time to form 2% polymer" in hours,

$$t = [Pu_T]^a[HNO_3]^b\, A e^{c/T},$$

where a = -1.6, b = 4.6, c = 12,300 K, and A = 7.66×10^{-16} h $\underline{M}^{-3}$; $[Pu_T]$ is the total plutonium concentration, mol/L; and $[HNO_3]$ is the makeup nitric acid concentration, mol/L.

---

1. INTRODUCTION

Over the past several years, the chemistry of Pu(IV) hydrous polymer has been actively studied in this laboratory in order to determine the effects of various conditions on the kinetic mechanisms involved. Originally, our interests lay with the influence of uranyl nitrate on the polymer formation rate,[1,2] whereupon the study progressed to an examination of the effects of reflux on the polymer chemistry.[3] With all of these accumulated data on the polymer kinetics, it was considered timely to derive a general model that would permit a prediction of the polymer kinetics over a broad range of conditions. Therefore, we have sought to derive a mathematical expression that would fit the previous data and could also be extrapolated beyond this range into regions that would be too difficult to study directly.

Although the ultimate goal of our work was to derive a mathematical function that would describe the polymer formation kinetics, development of the model and testing of the parametric relationships were important factors that could not be omitted. Therefore, the results are presented in a more-or-less chronological fashion. If the reader is interested in only the mathematical function, he can disregard much of this material and use the expression directly. We must emphasize that the model is an oversimplification of a complex mechanism; nevertheless, it is offered because it is reasonably accurate and is easy to use. The limitations have been collected in a final paragraph for convenient reference.

2. EXPERIMENTAL METHODS

The experimental approach used in this study was the same as that used earlier[1-3] and is thus described here only briefly. The results were typically obtained by monitoring Pu(IV) nitric acid solutions spectrophotometrically to determine the rate of change in the concentration of Pu(IV) hydrous polymer. This standard method also permitted the determination of the other plutonium species that were formed during the disproportionation of Pu(IV). Because the precision of the data depended so critically on the preparation and characterization of the solutions, much effort was given to careful handling of the solutions.

2.1 SOLUTIONS

The aqueous nitric acid solution of unhydrolyzed Pu(IV) was prepared just prior to each polymerization experiment by dissolving crystalline $Pu(NO_3)_4 \cdot xH_2O$ in cold HNO_3 solution so that the sum of the occluded acid in the crystalline reagent plus that of the solvent was equivalent to the desired "makeup"* value. The crystalline plutonium nitrate had been prepared earlier by taking a stock solution of Pu(IV) in approximately

*"Makeup nitric acid concentration," designated as $[HNO_3]$, represents the total acid added to the solution from both occluded acid in the crystalline stock and diluent acid in the solution. It does not include the acid generated in hydrolysis or disproportionation reactions, however. Real acid concentrations, including the latter two sources, will be designated as $[HNO_3]_{real}$.

1 M HNO_3 to dryness and performing the necessary analytical work to determine the Pu(IV) concentration, as well as the occluded HNO_3 and water contents.[1,2] A typical "x" value was 3.6.

2.2 DISSOLUTION PROCEDURE

Under many conditions, the process of dissolving Pu(IV) reagent crystals produced local temperature and concentration gradients that resulted in the premature initiation of polymer. To minimize this occurrence, the solutions were prepared cold by dissolving the reagent in ice-chilled HNO_3 solutions; they were then warmed to the temperature of interest in an electrically heated copper block.

2.3 SPECTROPHOTOMETRIC ANALYSES

Progress of the polymerization reaction (along with that of other competing reactions such as disproportionation) was monitored by a Cary 14H or 17H absorption spectrophotometer. The solutions were examined in silica cells with pathlengths that varied from 0.5 to 5.0 cm, depending on the concentration of the plutonium solution under consideration. The temperature of each solution was controlled by enclosing the cell in a thermostated copper block. Absorption spectra were measured from 1300 to 350 nm, and concentrations of the various plutonium species were determined by the techniques described earlier.[1,2] The growth of the colloidally suspended polymer was monitored by following the increase in absorbance of the 400-nm shoulder characteristic of the polymer. The times to form given percentages of polymer could be determined from these measurements.

2.4 GRAPHICS AND COMPUTATIONAL METHODS

A new series of computer programs was developed for three-dimensional and two-dimensional plotting of experimental and computational data. The main plotting was accomplished through a series of FORTRAN-callable subroutines using DISSPLA[4] software. The plotting of experimental data also required a series of surface interpolation routines called CISURF.[5] From a series of irregularly spaced experimental points, the program generated a Thiessen triangular grid from which a rectangular grid conforming to selected increments of $[Pu_T]$ and $[HNO_3]$ was produced.

Interpolated values of log(2% times) were generated at these grid points and plotted by DISSPLA calls. Two-dimensional sections of either constant [Pu] or constant $[H^+]$ could be plotted by the selection of appropriate array subscripts.

3. RESULTS AND DISCUSSION

The first step in the development of a kinetic model should be the identification of all the parameters affecting the process in question. In the case of Pu(IV) hydrous polymer chemistry, these are: temperature; concentrations of the plutonium, HNO_3, NO_3^-, and UO_2^{2+}; and reflux vs nonreflux conditions.[3] The complexity of deriving a mathematical function that incorporates all of the above is overwhelming; and since a fairly good understanding of the $[UO_2^{2+}]$ and reflux parameters had already been obtained,[1-3] these were regarded as secondary factors to be considered after a more-quantitative model based on the other parameters had been developed. Another of the parameters, $[NO_3^-]$, is not treated here in any detail because of restrictions in the scope of this work. Nevertheless, some discussion about the complicated NO_3^- effect will be given, even though it is based on limited data. The three remaining parameters, T, [Pu], and $[HNO_3]$, were therefore selected as the variables to be examined in the present kinetic study. Although such a study could involve extensive work, it was anticipated that the previous results plus the data from a few additional experiments at selected conditions would suffice for the establishment of a practical model.

Kinetic data are typically represented in the form of a rate expression, d[concentration]/dt; but in the case of plutonium polymer chemistry, the mechanisms of hydrolysis, aggregation (which is often preceded by an induction period), and aging are too complex to represent in completely rigorous fashion. To avoid confusion about the measured kinetics, the rate expression was replaced by the measured quantity of greatest significance — "time to form polymer" — because this is the point at which a problem would develop in a fuel reprocessing stream.

The polymer detection limit using the spectrophotometric method was at ~1% of the total plutonium in the system. This is true for all

concentrations since the cell pathlength was normally varied to keep the absorption bands of all plutonium species at suitably measurable intensities. Therefore, a value of 2% was arbitrarily selected as the most accurately identifiable minimum polymer concentration and the earliest stage at which polymer formation could be routinely and quantitatively identified.

Before proceeding further, it must be emphasized that an inverse relationship exists between the conventional rate expression and the "time to form 2% polymer." Qualitatively, it is easy to visualize that increasing the $[HNO_3]$ would decrease the rate of polymer formation and, in other words, increase the time to form the measurable amount of polymer. Although the time to form 2% polymer (hereafter called "2% time") will be developed into a mathematical expression, continual reference to kinetic rates of polymer formation will also be made during the course of the discussion. Confusion about whether the polymer formation rate follows a $-n$th order or the 2% time follows a $+n$th order in some variable (e.g., HNO_3) should be avoided.

Times to form 5 and 10% polymer were also determined prior to the termination of each experiment; but since the appearance of polymer was of prime concern here, no use of these additional data has been made thus far.

3.1 DEVELOPMENT OF MODEL

Initially, a graphical method was used to generate an overall profile of the data and thereby examine the scatter of the individual points. Three-dimensional plots of log(2% time) vs total plutonium concentration, $[Pu_T]$, and makeup nitric acid concentration, $[HNO_3]$, were made for data at a given temperature. The log(2% time) presentation was chosen in order to present the widely varying times required to produce 2% polymer. This range extended from minutes to days for the particular conditions selected. Although even shorter or longer times were also achievable by adjustment of the solution conditions, it was not practical to pursue these extremes with the spectrophotometric method.

The three-dimensional plot of the 25°C data (20 points) is shown in Fig. 1 for $[Pu_T]$ = 0.01 to 0.125 M and $[HNO_3]$ = 0.07 to 0.25 M. An

ORNL-DWG 83-8728

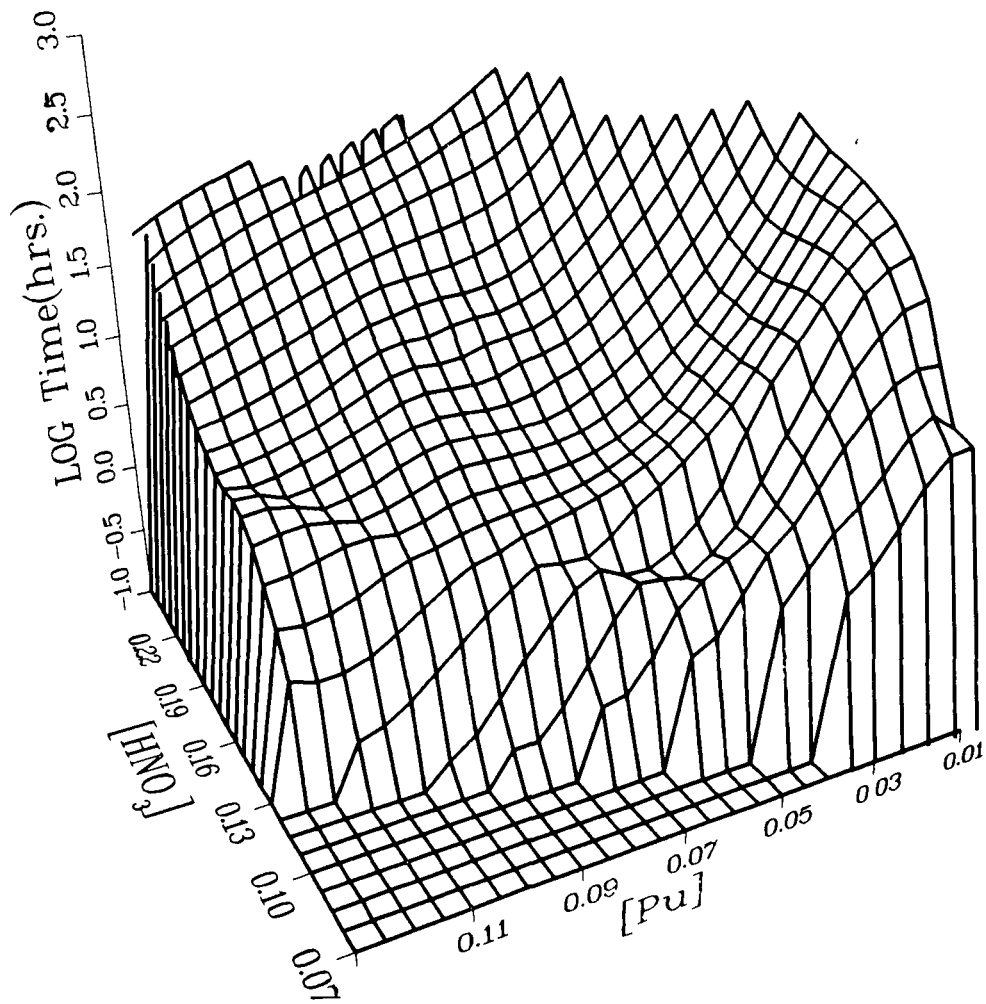

Fig. 1. Three-dimensional plot of real data: log(time to form 2% polymer, in hours) vs concentrations of total plutonium, [Pu_T], and makeup acid, [HNO_3], at 25°C after applying a smoothing routine to obtain a uniform surface.

interpolation routine was used between the points to produce a continuous surface, but the scatter in the data is still evident from the irregularities in the plot. Points on the curved surface represent the times to form 2% polymer for a given set of $[Pu_T]$ and $[HNO_3]$ values, while the grid in the plane at log(t) = -1.0 and the nearly vertical lines connecting log(t) = -1.0 and the curved surface are included to assist in visualizing the nature of the surface. Because the figure is drawn in perspective, the intervals between grid points do not appear to be regular. The aspect of viewing the figure should also be noted because the front corner represents conditions of lowest $[HNO_3]$ and highest $[Pu_T]$ and, therefore, the shortest 2% times. This aspect produces a three-dimensional figure in which all points of the curved data surface are visible and are not shadowed by other points.

Similar plots of data at 50°C (Fig. 2) and 70°C (Fig. 3), 16 and 11 points, respectively, were made on the same coordinate system. Although the scatter in the data increases to a great extent in these figures, the trend to shorter times with increasing temperature is readily seen.

A two-step approach was used in the course of analyzing these data at the various temperatures. First, a formal analysis of the data was made to determine the exact orders of the reaction with respect to the variables in question and the value of the activation energy for the polymer formation reaction. For this purpose, $[Pu_T]$ and $[HNO_3]$ (i.e., makeup acid concentrations) were not adequate; instead [Pu(IV)] and real nitric acid concentrations were necessary. Then, after completion of the formal analyses that unambiguously demonstrated the overall behavior, a general, simplified mathematical model was developed for practical applications.

3.2 DETAILED ANALYSIS

3.2.1 Order of Polymer Formation Reaction with Respect to $[HNO_3]$

To determine the order of the reaction* with respect to $[HNO_3]$, Fig. 4 was plotted from the 25°C data at both 0.01 and 0.05 M $[Pu_T]$. Using $[HNO_3]$

---

*Realizing that if the rate of reaction, $d[P]/dt = k[Pu]^m[HNO_3]^n$, then $\log\{d[P]/dt\} = \log k + m \log[Pu] + n \log[HNO_3]$ and the slope of a plot of the log(rate) vs log[concentration] would give the order, n or m, of the reaction with respect to that variable, Note: log(rate) $\propto$ -log(2% time).

ORNL-DWG 83-8729

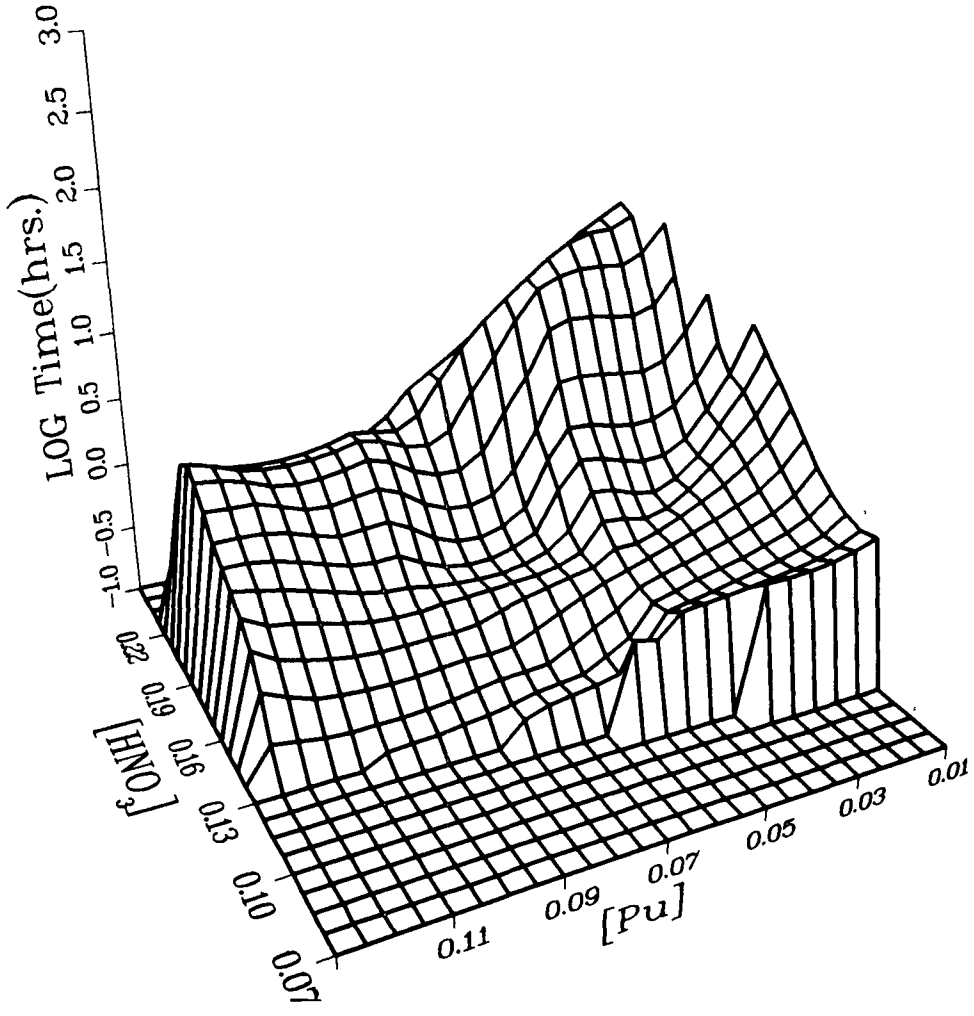

Fig. 2. Three-dimensional plot of real data: log(time to form 2% polymer, in hours) vs concentrations of total plutonium, [Pu_T], and makeup acid, [HNO_3], at 50°C after applying a smoothing routine to obtain a uniform surface.

ORNL-DWG 83-8730

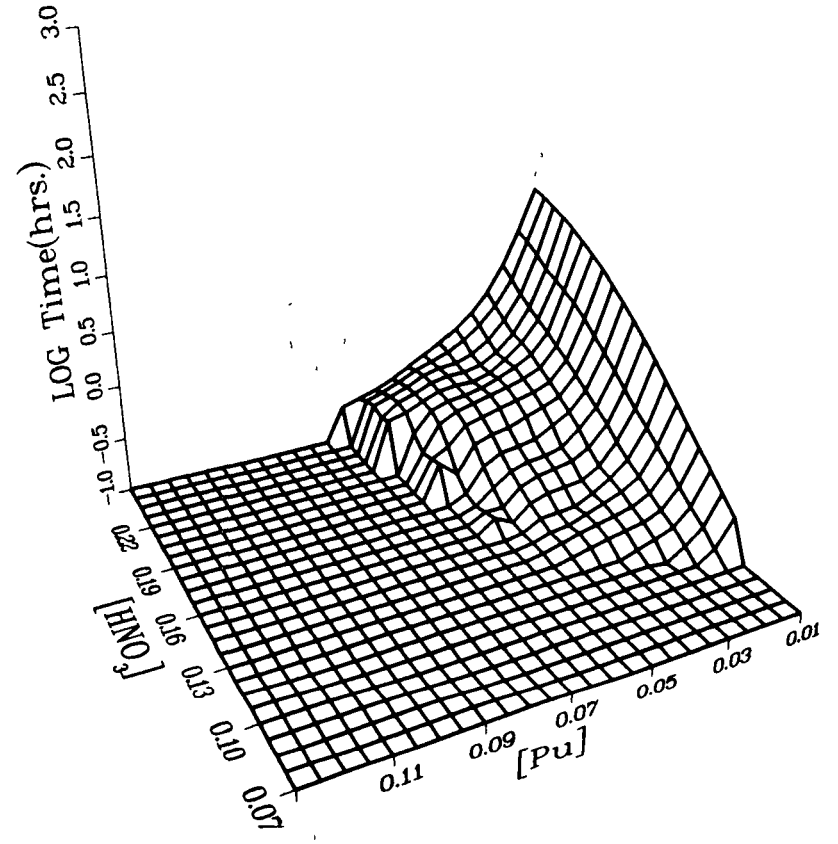

Fig. 3. Three-dimensional plot of real data: log(time to form 2% polymer, in hours) vs concentrations of total plutonium, [Pu_T], and makeup acid, [HNO_3], at 70°C after applying a smoothing routine to obtain a uniform surface.

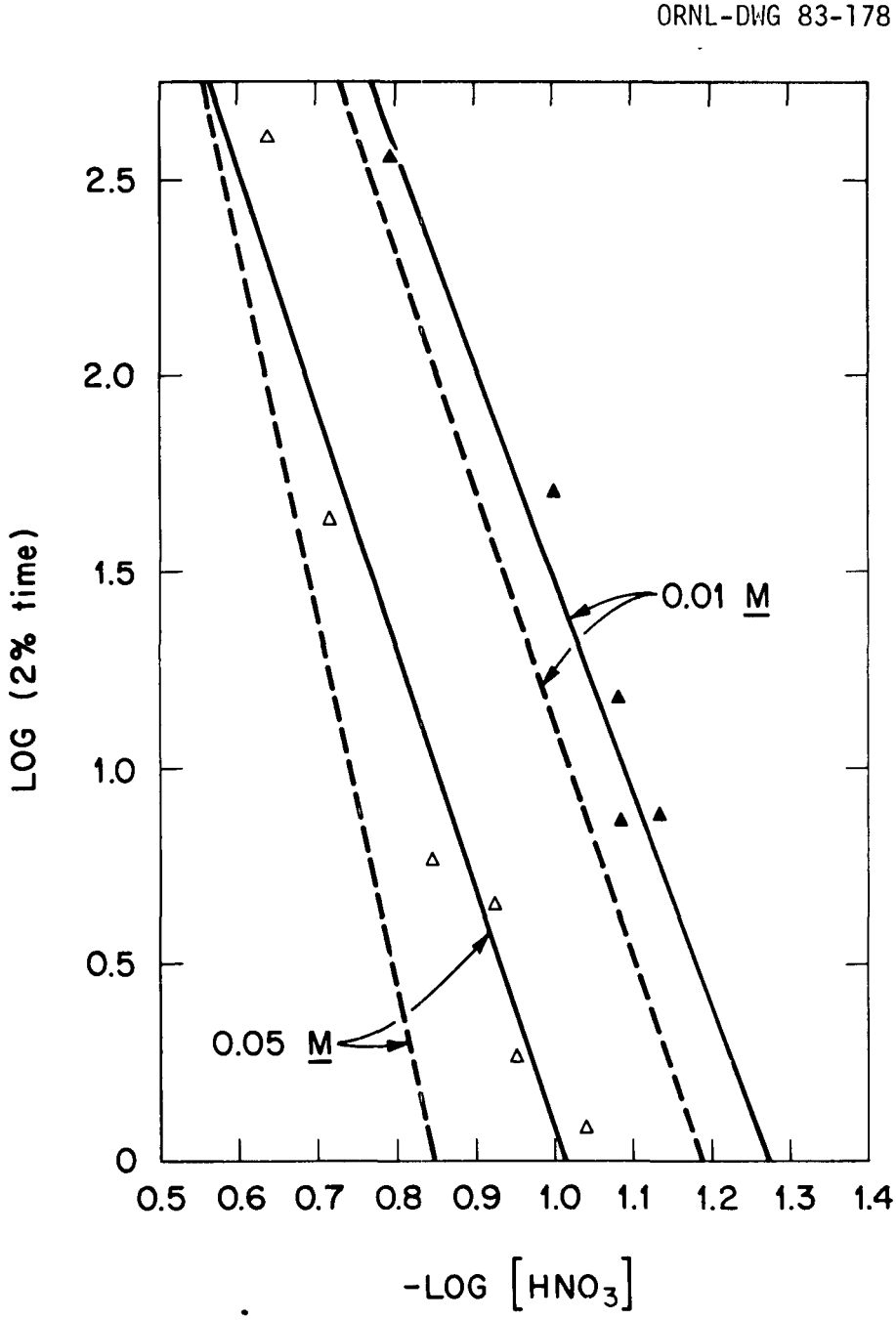

Fig. 4. Determination of the order of the polymer formation reaction with respect to $[HNO_3]$ for 0.01 and 0.05 M plutonium at 25°C. Solid lines and data points are for makeup acid values, whereas accompanying dashed lines are for calculated real acid values.

(i.e., makeup values), the solid lines were obtained for the two respective concentrations. The slopes of these lines were -5.5 and -6.1, respectively, suggesting to a first approximation that the rate of polymer formation was ~6th order in $[HNO_3]$. Realizing, though, that the makeup acid values did not represent the true acid concentration of the solution, a correction was made for the acid formed as a result of Pu(IV) disproportionation with no identifiable Pu(V):

$$3Pu^{4+} + 2H_2O \rightleftarrows 2Pu^{3+} + PuO_2^{2+} + 4H^+ . \qquad (1)$$

By spectrophotometrically determining the concentrations of the three plutonium oxidation states, the additional acid contributed to the system via the above reaction could be computed and added to the makeup values.

When these corrected acid concentrations were plotted in Fig. 4 (see the dashed lines), slopes of 6.1 and 9.3 were obtained for the 0.01 and 0.05 M plutonium experiments, respectively. The discrepancy in the two values was indicative of our inability to quantitatively calculate the acid concentrations in these experiments (based on a large experimental error in the determination of the various plutonium ion concentrations). Because the results obtained for 0.01 M plutonium would yield a smaller error in the acid values than those for the 0.05 M $[Pu_T]$, they were believed to yield the more accurate value for the order of the reaction with respect to $[HNO_3]$. Therefore, this value was assigned as -6.

3.2.2 Order of Polymer Formation Reaction with Respect to [Pu(IV)]

Results obtained in earlier work[3] indicated that the rate of polymer formation was first order in [Pu(IV)]. With this information and the previously determined -6th power $[HNO_3]$ dependency, an entire surface at a given temperature could be generated from a single data point. However, in order to generate plots for comparison with those of Figs. 1-3, which were in terms of $[Pu_T]$ instead of [Pu(IV)], some knowledge of the equilibrium quotient, Q, was required for the reaction in Eq. (1).

The equilibrium quotients were calculated from previously unpublished data that were similar in many respects to the values already reported.[6,7] The only difference was an apparent dependency of the equilibrium quotient on $[Pu_T]$. (These observations will be discussed in a subsequent report.) From the experimentally determined variation of Q as a function of $[Pu_T]$ at various temperatures, the times to form 2% polymer at given values of

[Pu(IV)] and $[HNO_3]_{real}$ could be converted to model plots of log(2% time) vs $[Pu_T]$ and $[HNO_3]$. Upon comparison of these plots with those of Figs. 1-3, it was apparent that a first-order dependency of the rate on [Pu(IV)] did not give as good a fit as a 1.2 order; therefore, the plots were corrected to represent a rate that was proportional to $[Pu(IV)]^{1.2}$ and $[HNO_3]^{-6}_{real}$. These plots, shown in Figs. 5-7, compare very favorably with those of the real data in Figs. 1-3, respectively.

It is not difficult to rationalize the 1.2 power dependency of the polymerization rate on [Pu(IV)] since polymer growth has been previously shown to follow a third-power dependency on [Pu(IV)] and the data indicating a 1.2 power for polymer formation could have included some small degree of polymer growth as well.

3.2.3 Activation Energy for Polymer Formation Reaction

The only aspect limiting the development of a general model was an activation energy for the formation reaction. Either the real data of Figs. 1-3 or the model of Figs. 5-7 could be used to construct Arrhenius plots for sets of values at fixed values of $[Pu_T]$ and $[HNO_3]$. (The model was preferred for this analysis because it represented a smoothed approximation of the actual data.) Unfortunately, neither approach yielded straight-line Arrhenius plots, suggesting that the data scattered badly or that the activation energy varied with temperature.

The data shown in Fig. 8 were measured to determine if the activation energy did vary with temperature. Two different acid concentrations were used to enable a scaling of the reaction conditions to reasonable time values (i.e., for times that varied from log(t) of -1.0 to 1.5, or 0.1 to 32 h). Despite this necessity, the results clearly show that a considerable increase in the activation energy does occur with increasing temperature. Although straight-line segments were drawn through these data, the error in the measurement was sufficient to allow a continuous, smooth line instead. The line segments were used merely to emphasize the change in the activation energy by their slopes.

An increase in the activation energy with increasing temperature is not surprising when it is realized that the polymer formation mechanism involves a complex number of reactions, including hydrolysis, aggregation,

ORNL-DWG 83-8731

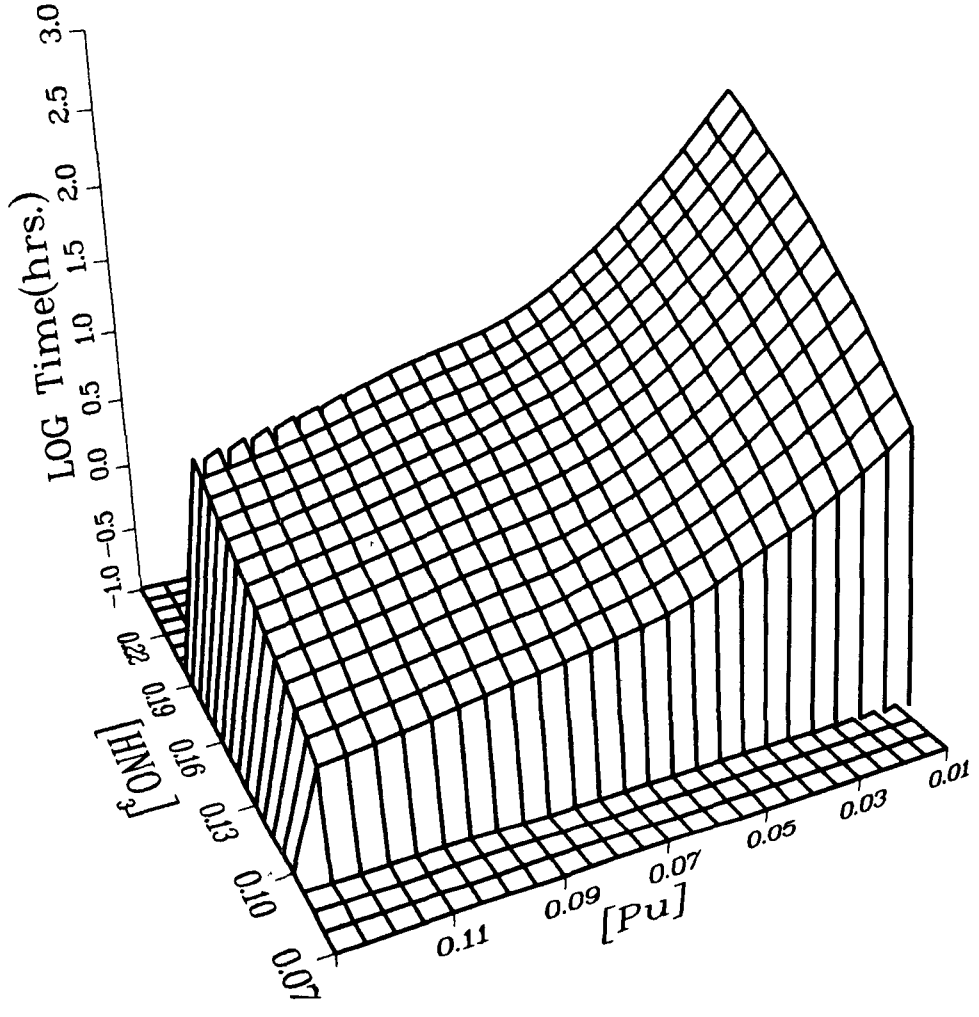

Fig. 5. Three-dimensional plot of log(time to form 2% polymer, in hours) vs concentrations of total plutonium, $[Pu_T]$, and makeup acid, $[HNO_3]$, at 25°C using model: $\log(t) \propto [H^+]^6[Pu(IV)]^{-1.2}$.

ORNL-DWG 83-8732

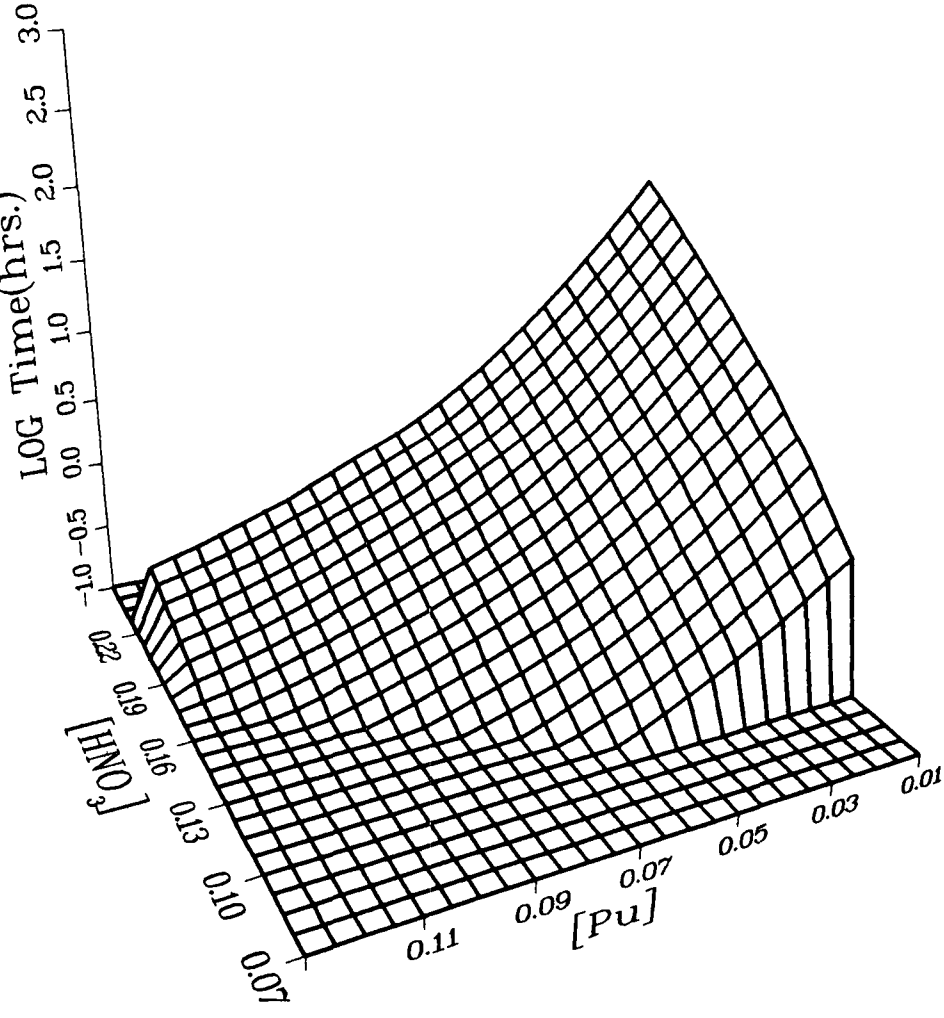

Fig. 6. Three-dimensional plot of log(time to form 2% polymer, in hours) vs concentrations of total plutonium, $[Pu_T]$, and makeup acid, $[HNO_3]$, at 50°C using model: $\log(t) \propto [H^+]^6[Pu(IV)]^{-1.2}$.

ORNL-DWG 83-8733

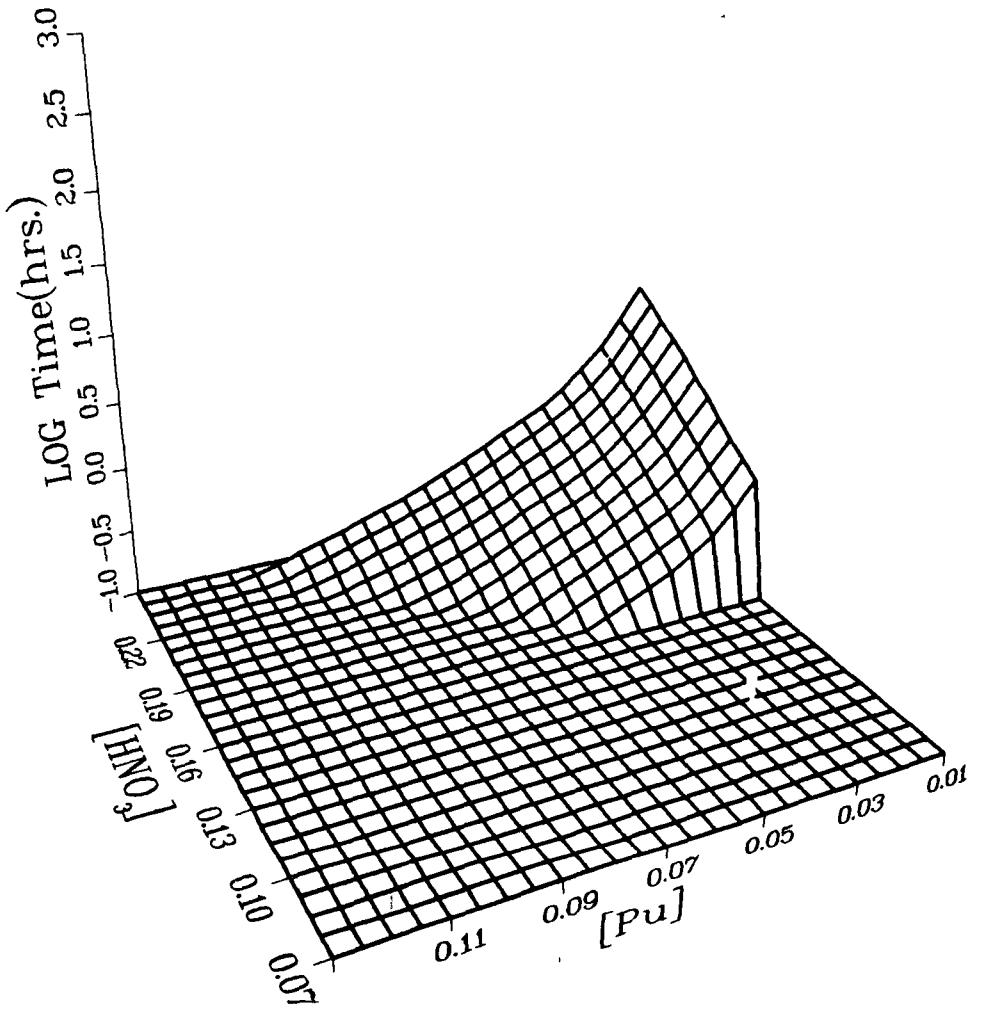

Fig. 7. Three-dimensional plot of log(time to form 2% polymer, in hours) vs concentrations of total plutonium, $[Pu_T]$, and makeup acid, $[HNO_3]$, at 70°C using model: $\log(t) \propto [H^+]^{6+}[Pu(IV)]^{-1.2}$.

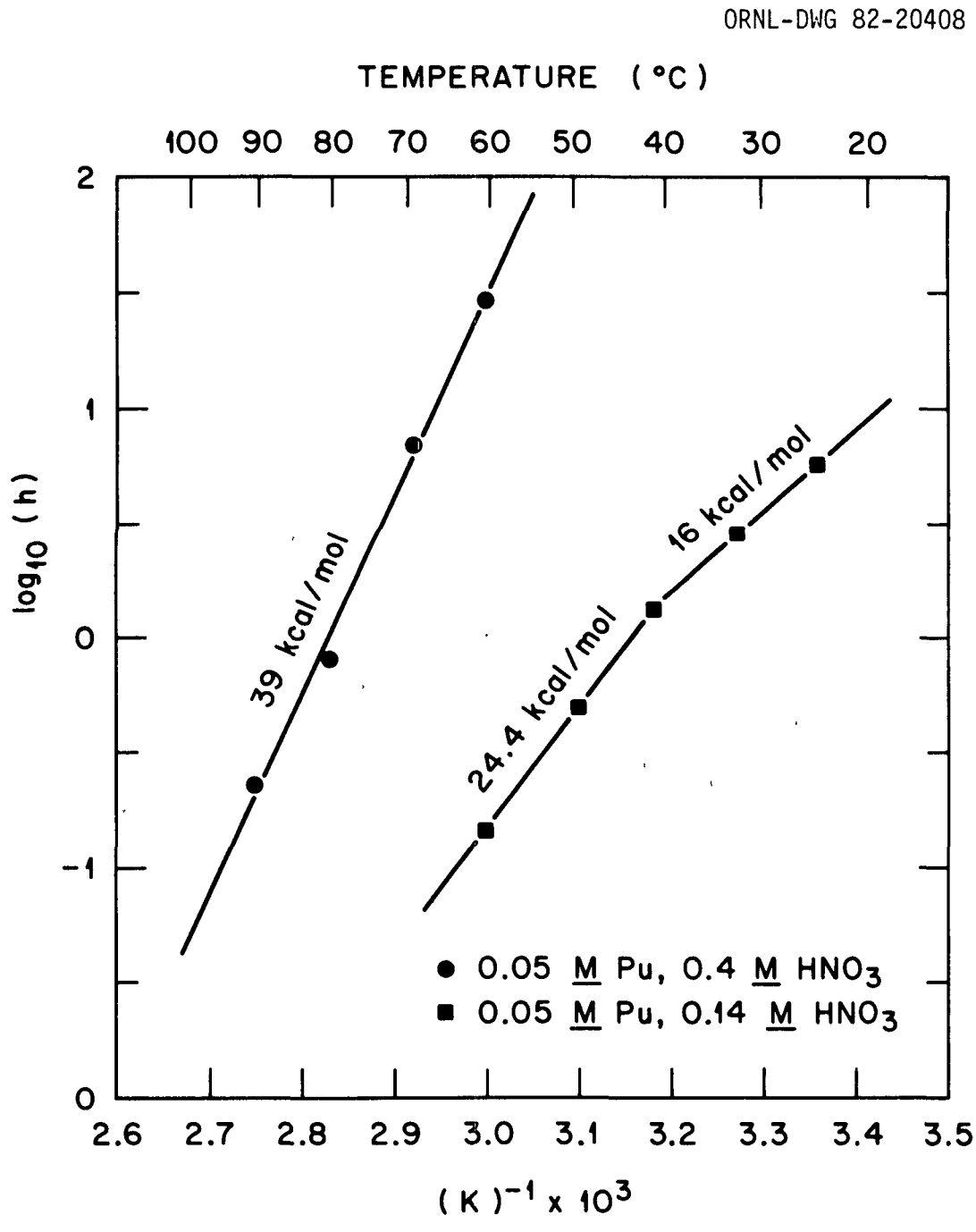

Fig. 8. Arrhenius plot showing variation of activation energy for Pu(IV) polymerization with temperature.

and aging, all of which vary significantly with temperature. Consequently, the rate-determining step could also change with temperature and, therefore, alter the magnitude of the measured activation energy.

Using the 163.2-kJ/mol (39-kcal/mol) value for the activation energy for the 70 to 105°C region, we can estimate the 2% time for $[Pu_T]$ = 0.05 M and $[HNO_3]$ = 1.0 or 2.0 M. Starting with a 2% time of 0.3 h for $[Pu_T]$ = 0.05 M and $[HNO_3]$ = 0.206 M at 70°C, the sixth-power acid dependency followed by the change in rates due to the temperature can be computed to yield calculated times of 13 and 708 h as compared with 18 and 191 h (measured) for the respective 1.0 and 2.0 M HNO_3 solutions at 105°C. The agreement is quite reasonable for the model at this stage, considering that only a single given starting point was used.

3.3 GENERALIZED MATHEMATICAL MODEL

Having established that the rate of polymer formation is −6th order in $[HNO_3]$ and +1.2 order in [Pu(IV)] and has an activation energy that varies from 66.9 to 163.2 kJ/mol (16 to 39 kcal/mol), it would seem to be a simple matter to incorporate these into a concise mathematical expression. However, two concerns dominate the further development of a practical model: (1) the orders of the reaction depend on a knowledge of $[Pu(IV)]/[Pu_T]$, which is cumbersome to determine; and (2) the major goal of this work was to derive a simple model that predicted polymer appearance times without regard to all of the intervening redox chemistry, especially Pu(IV) disproportionation. Therefore, a purely empirical model would be just as acceptable if it predicted polymer formation; the empirical model would be ideal if it were also physically realistic.

A least squares routine[8] that would solve either linear or nonlinear functions was used to test various mathematical models. The best fit of all the experimental data was obtained with the following function:

$$t = [Pu_T]^a [HNO_3]^b \, e^{(c+dT)/T} , \qquad (2)$$

where t is the 2% time in hours; T is the absolute temperature; $[Pu_T]$ is the total plutonium concentration; $[HNO_3]$ is the makeup acid concentration; and a, b, c, and d are adjustable parameters. The least squares routine was actually performed on the logarithmic version of Eq. (2) because the

expression became linear and therefore converged more readily. The data used in the least squares fit are given in Table 1, along with the observed and calculated values of 2% time. Note that even the 105°C data are included from the previously published reflux study.[3] The least squares fit of the data produced the following values for the parameters in the above equation: a = -1.6, b = 4.6, c = 12,300 K, and d = -34.8. A plot of the residuals [i.e., $\ln(t_{obs}) - \ln(t_{calc})$] shows (Fig. 9) that the maximum error in the fit is ±1.73. In other words, from this plot and/or a comparison of $t_{obs} - t_{calc}$, it can be seen that the calculated times are generally within a factor of 2 of the observed times.

It should be immediately obvious that the parameters in the above empirical function do not correspond to the measured orders of the reaction discussed in the previous sections. On the other hand, it should be noted that these parameters are for $[Pu_T]$ and "makeup" nitric acid values, $[HNO_3]$, whereas the orders of the reaction determined earlier were for [Pu(IV)] and $[HNO_3]_{real}$. It should also be noted that a temperature-dependent activation energy term is not included in the expression because it did not markedly improve the fit of the data. (Variations in the model are discussed later in this section.)

Even though the model is empirical, it retains a degree of realism that is useful in understanding the polymerization mechanism. An example of this is evident if the form of Eq. (2) is rewritten as

$$t = [Pu_T]^a[HNO_3]^b A e^{c/T} , \qquad (3)$$

where the $A = e^d = 7.66 \times 10^{-16}$ h M^{-3} term would be equivalent to a pre-exponential factor such as that found in typical rate constant expressions and would have units, in this case, of h $\underline{M}^{-3}$ because of the fortuitous cancellation of fractional reaction orders. The "c" term would be equivalent to E*/R (the activation energy and the quotient of the gas constant), or E* = R·c = 102.3 kJ/mol (24.6 kcal/mol), which is a value similar to that found in Fig. (8) during the formal analysis of the data.

Three-dimensional plots of the function in Eq. (2) for 25, 50, and 70°C are shown in Figs. 10-12, respectively, followed by selected two-dimensional plots, Figs. 13-18, representing slices through the 3-D figures. The two-dimensional figures give a more quantitative appreciation of the trends with respect to the individual variables.

Table 1. Comparison of measured and calculated[a] values of "time to form 2% polymer" for 67 sets of conditions where $[Pu_T]$, $[HNO_3]$, and temperature were varied

2% time (n)		Concentration		Temperature (K)
Observed	Calculated	$[Pu_T]$	$[HNO_3]$	
5.80	17.74	0.002	0.050	298
311.23	114.49	0.002	0.075	298
7.50	9.40	0.010	0.077	298
7.38	12.55	0.010	0.082	298
50.0	31.27	0.010	0.100	298
354.80	279.53	0.010	0.161	298
18.00	6.89	0.020	0.092	298
1.30	1.22	0.035	0.077	298
3.00	1.93	0.035	0.085	298
1.20	1.47	0.050	0.091	298
1.82	3.68	0.050	0.111	298
4.40	5.06	0.050	0.119	298
5.80	11.79	0.050	0.143	298
42.70	45.70	0.050	0.192	298
407.40	102.79	0.050	0.229	298
1.85	2.82	0.090	0.129	298
31.55	23.72	0.090	0.205	298
0.44	1.33	0.125	0.123	298
2.28	3.30	0.125	0.150	298
3.65	3.51	0.125	0.152	298
21.00	6.89	0.125	0.176	298
9.55	13.58	0.125	0.204	298
66.10	32.14	0.125	0.246	298
2.92	3.63	0.050	0.140	306
1.32	1.30	0.050	0.140	314
1.33	1.22	0.010	0.099	323

Table 1. (continued)

2% time (n)		Concentration		Temperature (K)
Observed	Calculated	$[Pu_T]$	$[HNO_3]$	
1.37	1.28	0.010	0.100	323
10.00	15.04	0.010	0.171	323
1.67	3.38	0.025	0.171	323
18.50	11.00	0.025	0.221	323
5.90	13.22	0.025	0.230	323
0.70	0.14	0.050	0.109	323
0.50	0.44	0.050	0.140	323
2.00	1.19	0.050	0.174	323
0.22	0.13	0.061	0.116	323
0.78	1.00	0.061	0.180	323
0.67	1.34	0.090	0.220	323
0.40	0.28	0.092	0.158	323
0.18	0.10	0.113	0.137	323
0.09	0.24	0.125	0.170	323
0.33	0.78	0.125	0.220	323
0.32	0.78	0.125	0.220	323
1.60	3.26	0.125	0.300	323
3.12	6.63	0.125	0.350	323
0.17	0.07	0.128	0.133	323
0.15	0.14	0.050	0.140	333
36.43	17.34	0.050	0.400	333
0.38	0.43	0.005	0.100	343
35.50	28.85	0.005	0.250	343
0.18	0.14	0.010	0.100	343
11.80	6.36	0.010	0.230	343
0.40	0.39	0.020	0.160	343
1.60	1.68	0.020	0.220	343
2.68	2.50	0.020	0.240	343
0.12	0.09	0.050	0.160	343
0.39	0.56	0.050	0.240	343

Table 1. (continued)

2% time (n)		Concentration		Temperature (K)
Observed	Calculated	$[Pu_T]$	$[HNO_3]$	
6.90	5.90	0.050	0.400	343
0.10	0.03	0.051	0.130	343
0.38	0.22	0.051	0.197	343
0.22	0.33	0.070	0.240	343
0.25	0.57	0.050	0.300	353
0.80	2.13	0.050	0.400	353
11.35	13.76	0.050	0.600	353
0.23	0.82	0.050	0.400	363
18.00	14.34	0.050	1.000	378
191.00	347.64	0.050	2.000	378
97.00	17.48	0.550	2.440	378

[a]Using Eq. (2).

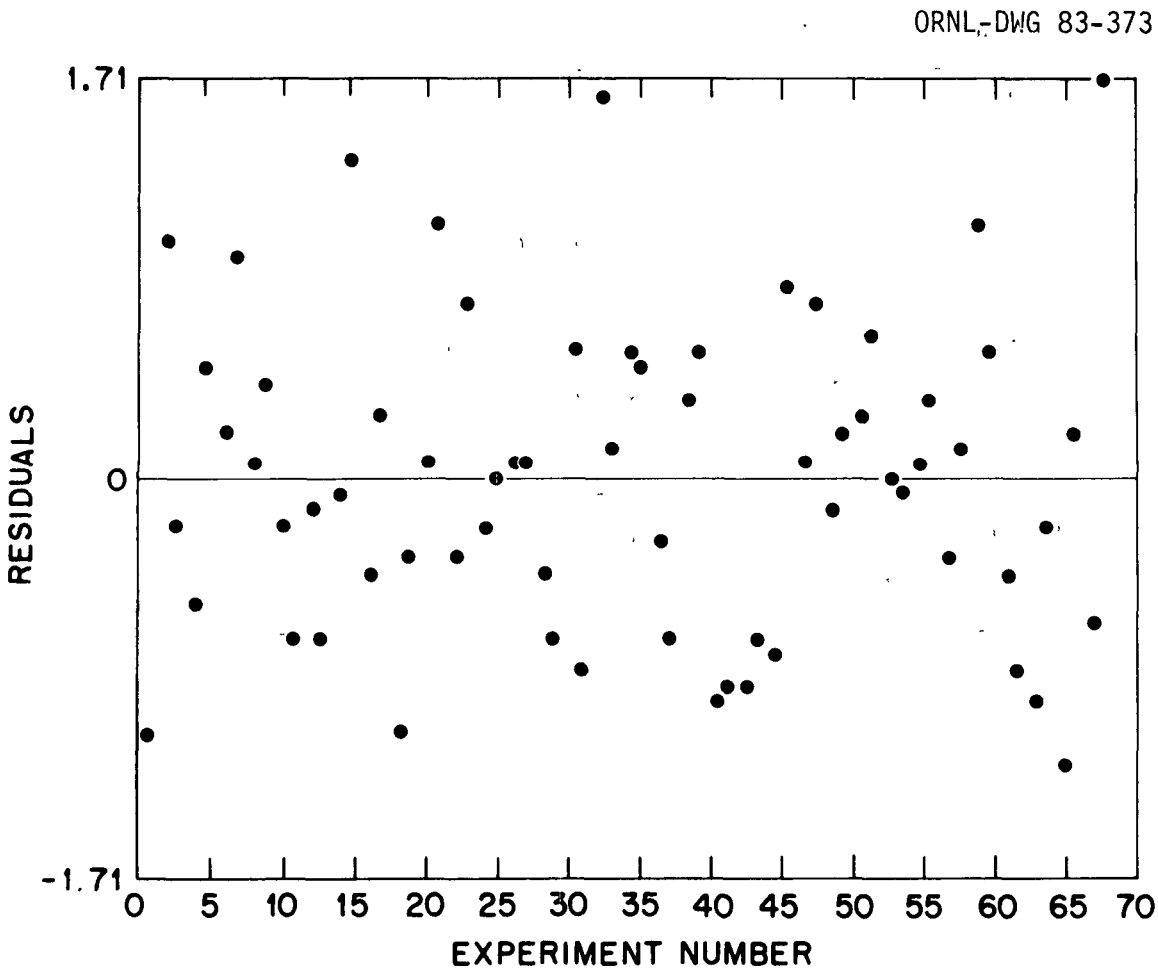

Fig. 9. Plot of residuals, $\log(t_{calc}) - \log(t_{obs})$, using the function of Eq. (2) for the 67 sets of data points given in Table 1. Note that these residuals are obtained by taking the difference of the logarithms of the values in columns 1 and 2.

ORNL-DWG 83-8734

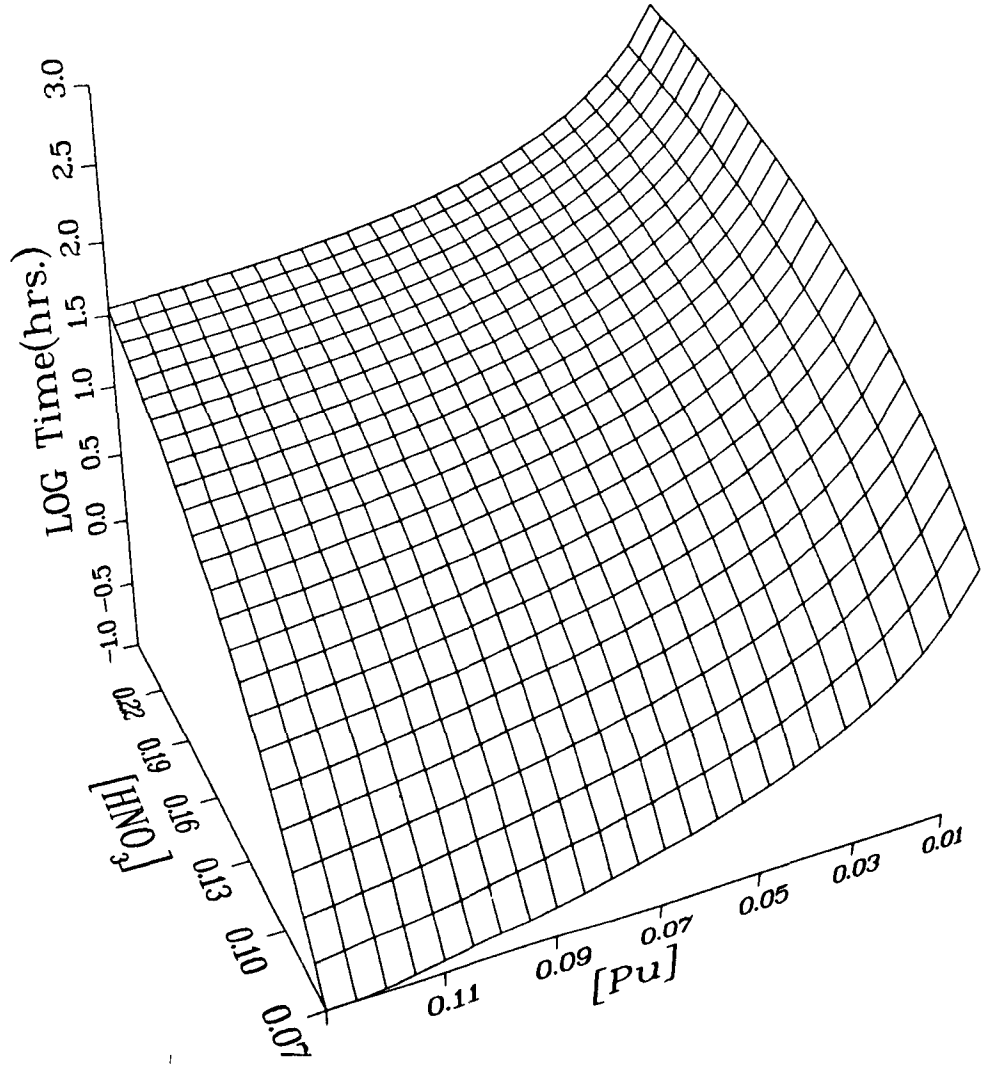

Fig. 10. Three-dimensional plot of log(time to form 2% polymer, in hours) vs concentrations of total plutonium, $[Pu_T]$, and makeup acid, $[HNO_3]$, at 25°C using function: $t = [Pu_T]^a[HNO_3]^b e^{(c+dT)/T}$, where a, b, c, and d are as defined in the text.

ORNL-DWG 83-8735

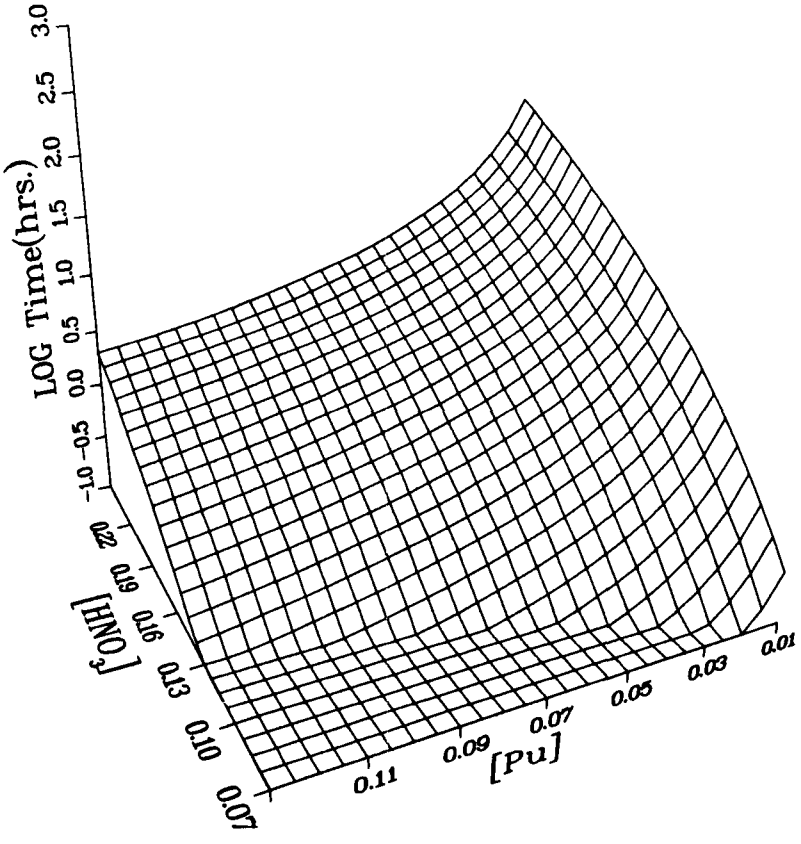

Fig. 11. Three-dimensional plot of log(time to form 2% polymer, in hours) vs concentrations of total plutonium, $[Pu_T]$, and makeup acid, $[HNO_3]$, at 50°C using function: $t = [Pu_T]^a[HNO_3]^b e^{(c+dT)/T}$, where a, b, c, and d are as defined in the text.

ORNL-DWG 83-8736

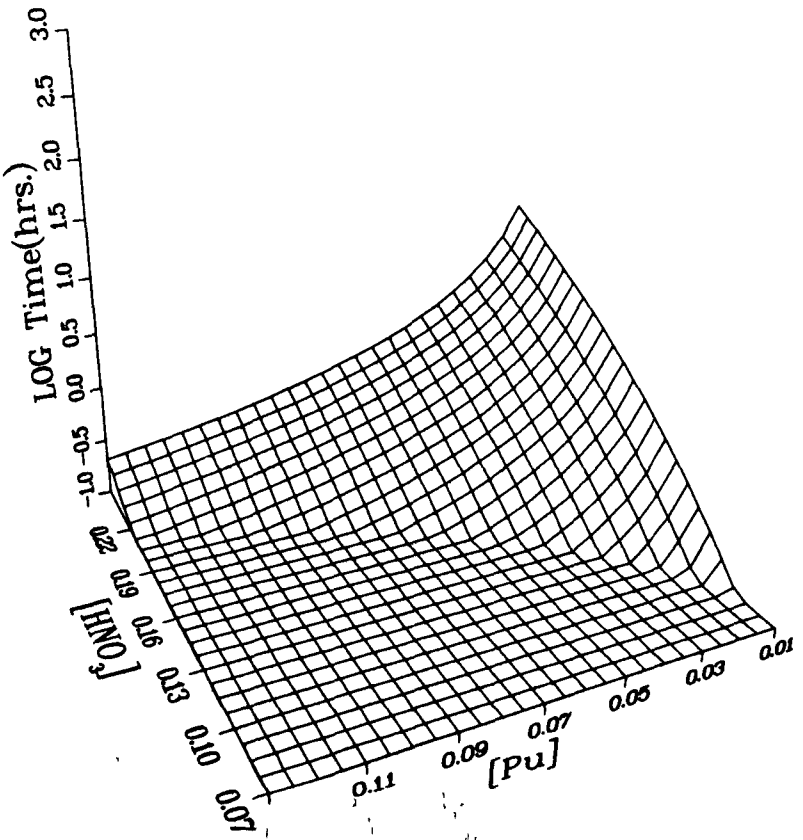

Fig. 12. Three-dimensional plot of log(time to form 2% polymer, in hours) vs concentrations of total plutonium, $[Pu_T]$, and makeup acid, $[HNO_3]$, at 70°C using function: $t = [Pu_T]^a[HNO_3]^b e^{(c+dT)/T}$, where a, b, c, and d are as defined in the text.

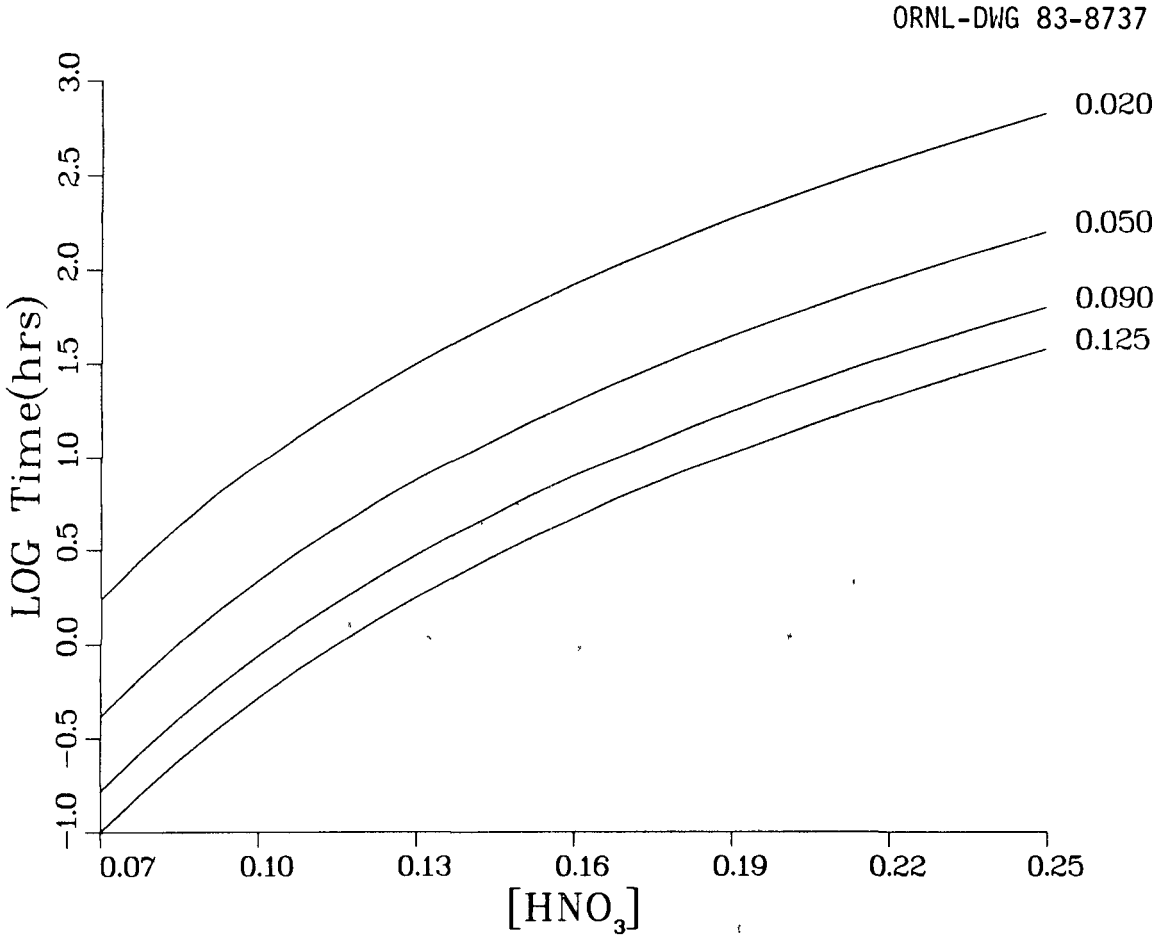

Fig. 13. Two-dimensional plot of function given in Eq. (2) for T = 298 K (25°C) at various fixed values of $[Pu_T]$, as indicated at extreme right of each curve.

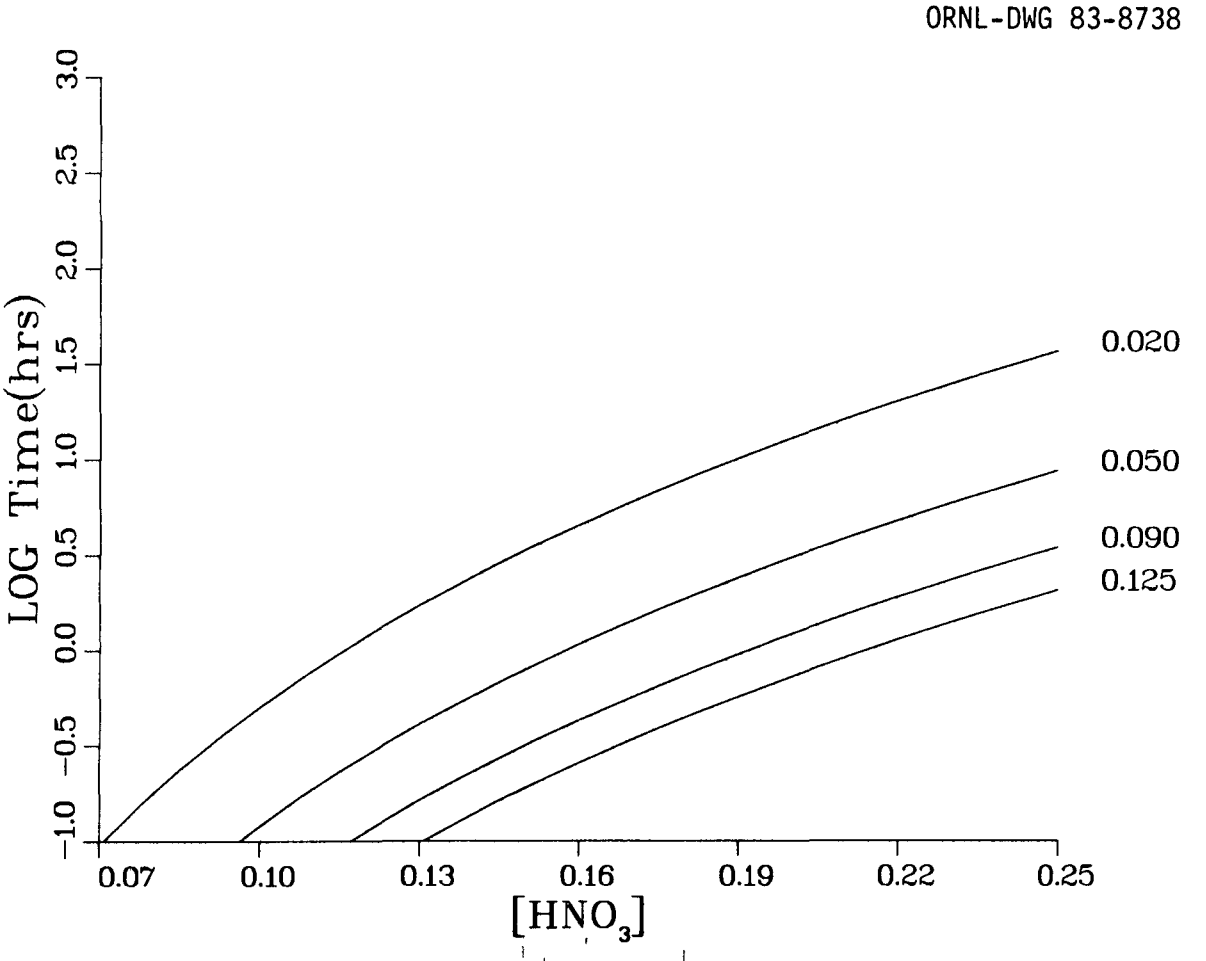

Fig. 14. Two-dimensional plot of function given in Eq. (2) for T = 323 K (50°C) at various fixed values of $[Pu_T]$, as indicated at extreme right of each curve.

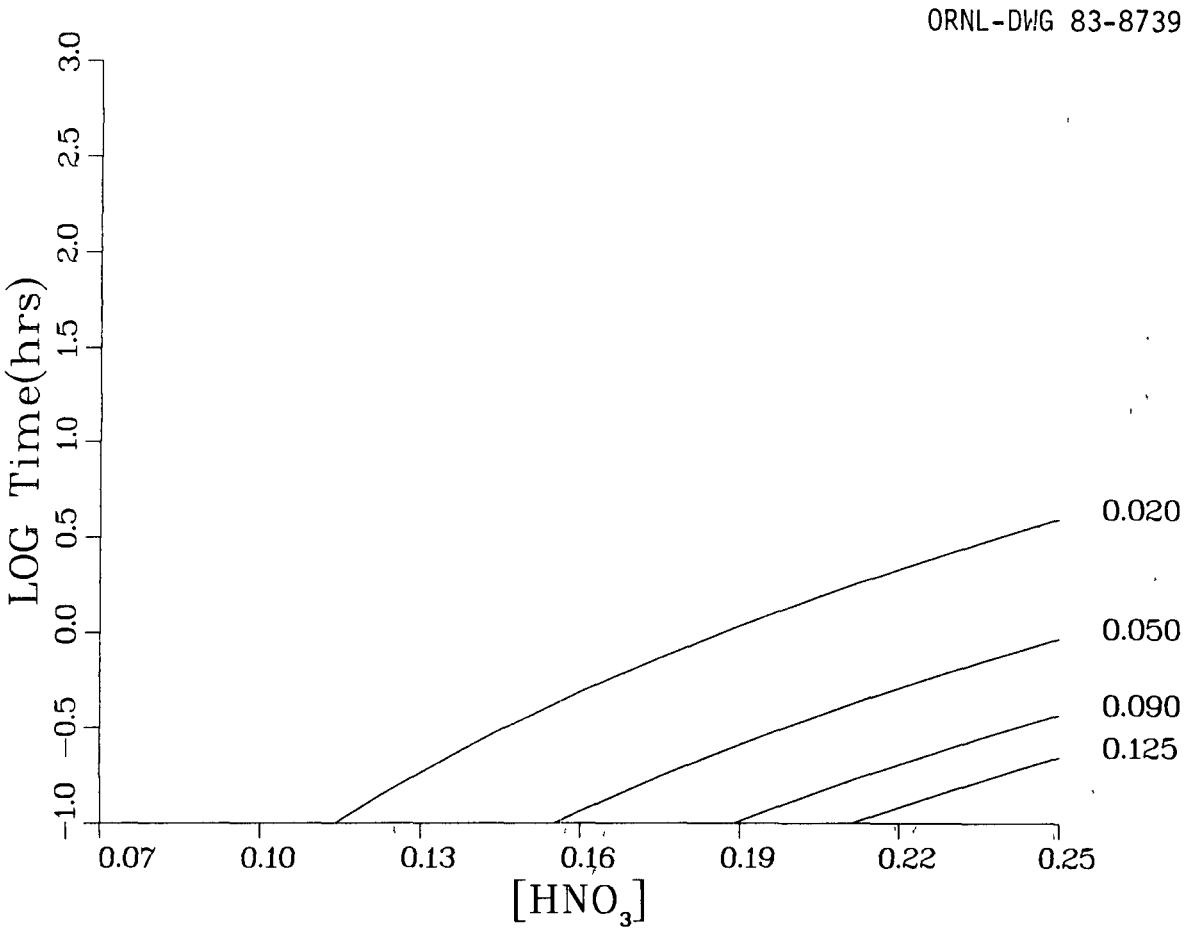

Fig. 15. Two-dimensional plot of function given in Eq. (2) for T = 343 K (70°C) at various fixed values of $[Pu_T]$, as indicated at extreme right of each curve.

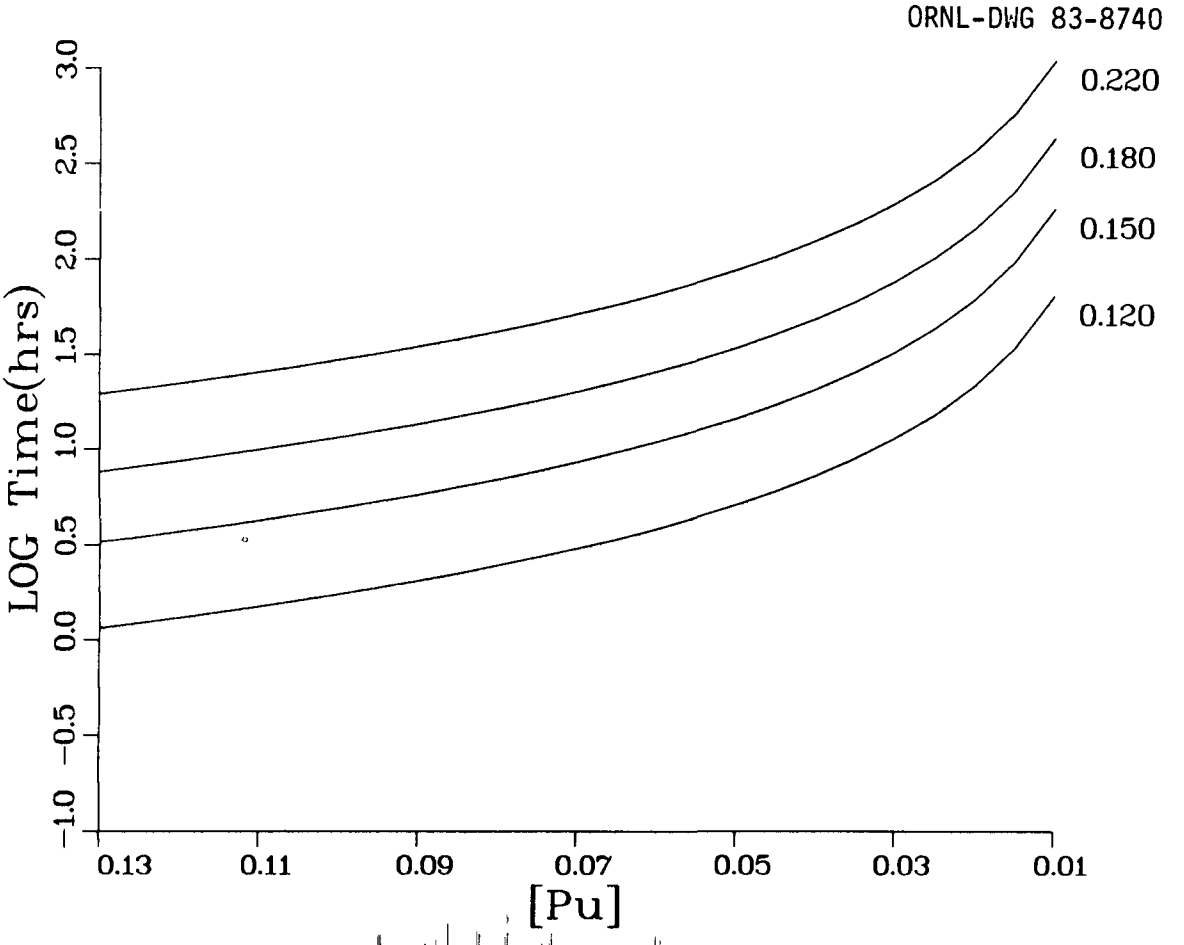

Fig. 16. Two-dimensional plot of function given in Eq. (2) for T = 298 K (25°C) at various fixed values of $[HNO_3]$, as indicated at extreme right of each curve.

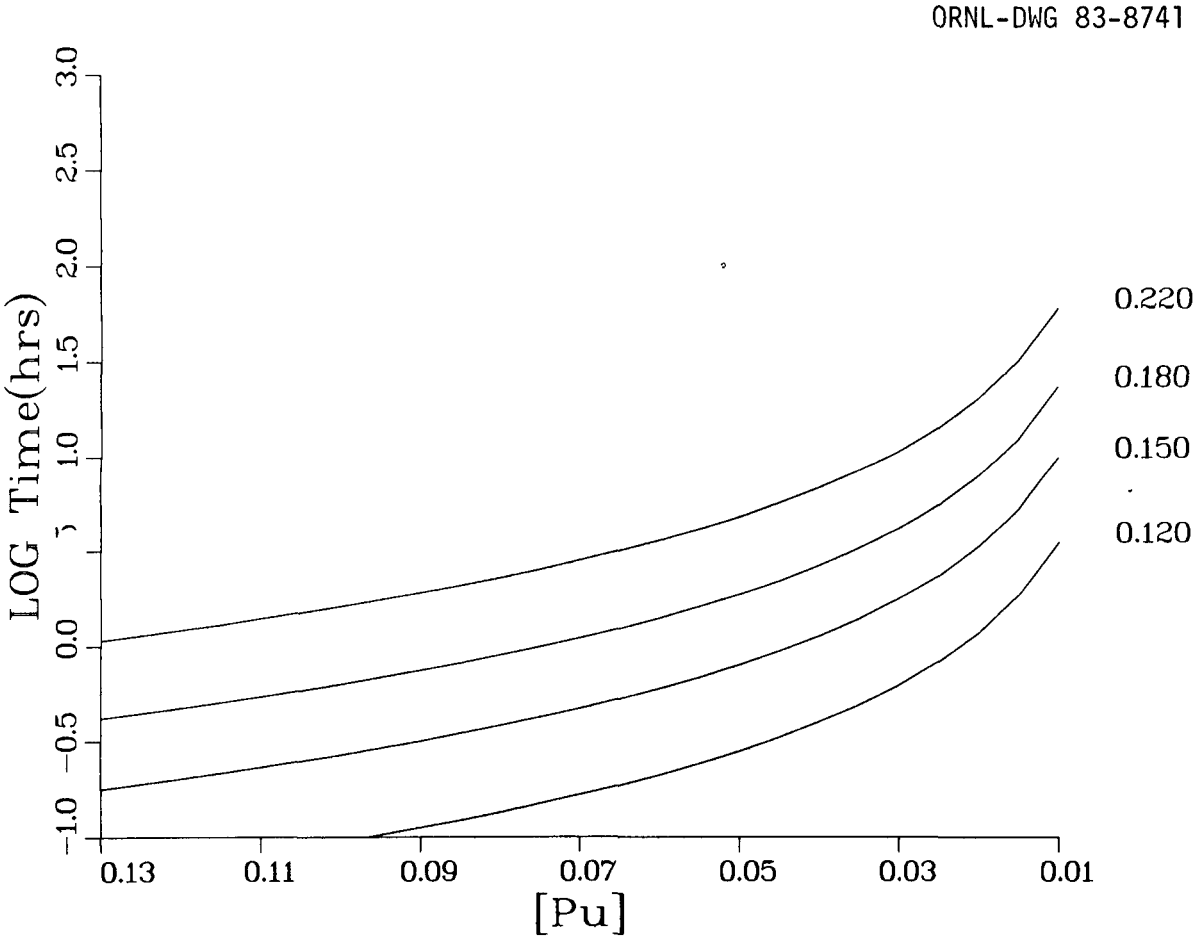

Fig. 17. Two-dimensional plot of function given in Eq. (2) for T = 323 K (50°C) at various fixed values of $[HNO_3]$, as indicated at extreme right of each curve.

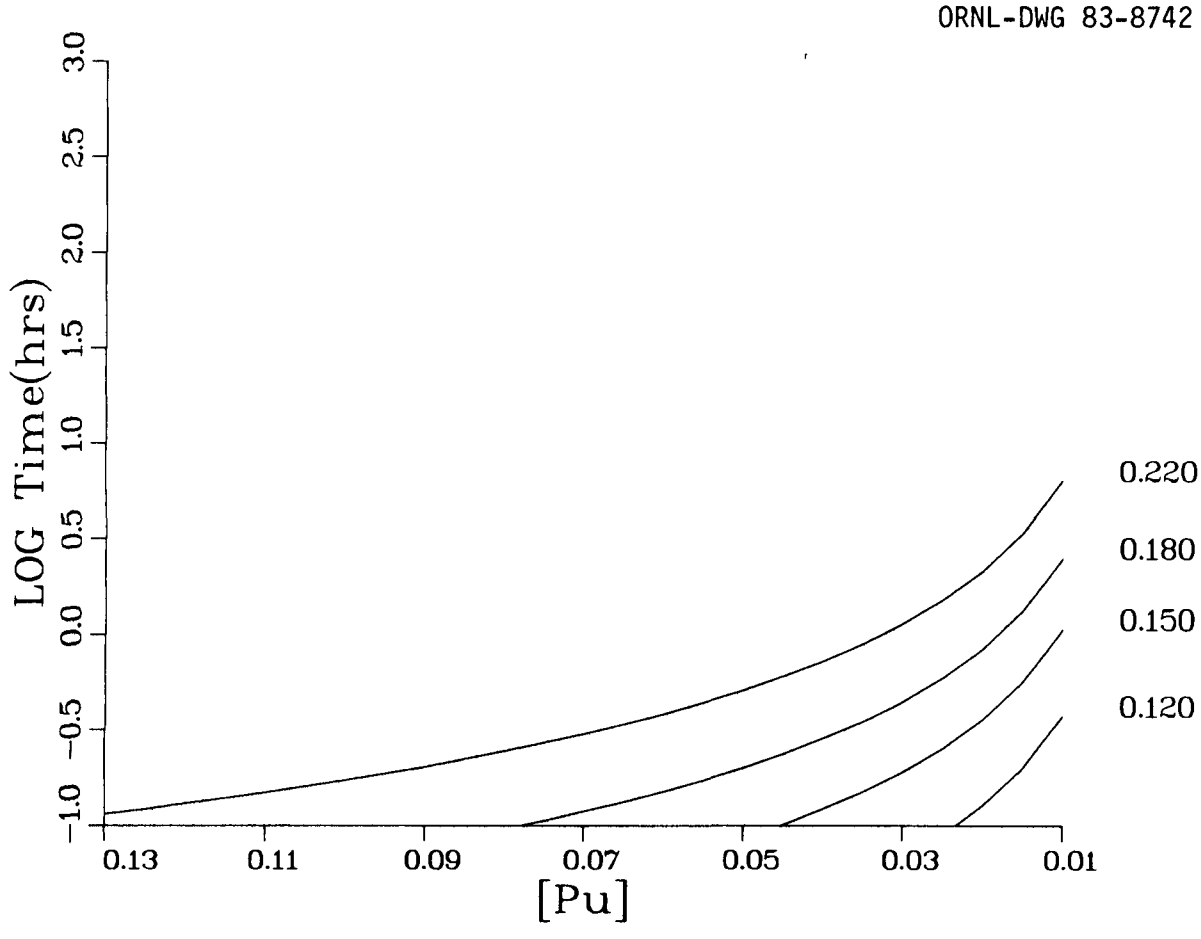

Fig. 18. Two-dimensional plot of function given in Eq. (2) for T = 343 K (70°C) at various fixed values of $[HNO_3]$, as indicated at extreme right of each curve.

Several variations of the mathematical model were examined and found to give almost comparable fits of the data. These are:

$$t = [Pu_T]^a[HNO_3]^b e^{(c+dT+fT^2)/T} , \quad (4)$$

$$t = [Pu_T]^a[HNO_3]^b T^f e^{(c+dT)/T} , \quad (5)$$

$$t = d[Pu_T]^a[HNO_3]^b[(T^* + 10)/100]^c . \quad (6)$$

The expressions given in Eqs. (4) and (5) demonstrate our attempts to include the observed temperature dependence of the activation energy, as shown in Fig. 8. In addition to the fT^2 term of Eq. (4), an f/T term was also tried, but no substantial improvement in the fit was obtained. The expression in Eq. (5) is a function similar to that used previously[9] to fit hydrolysis data and, like Eq. (4), provided no substantially better fit of the data.

The expression in Eq. (6) was suggested by Whatley.[10] The main difference between it and the other functions is the temperature term, which is given in Centigrade (T* notation used here) instead of Kelvin. As with the other models, however, it provides no improvement over the fit obtained with the function in Eq. (3).

In addition to representing times within the ranges covered by the actual data, the model can be employed in a predictive capacity by extrapolating beyond these typical acid conditions. Figures 19-22 show the effect of extreme ranges of $[HNO_3]$, from 0 to 3 M, on the times to form polymer at 25, 50, 70, and 100°C, respectively. Two different values for $[Pu_T]$ are plotted to indicate the effect of plutonium concentration. This series of figures demonstrates how significantly an increase in temperature will decrease the time to form polymer. For example, Fig. 22 shows that for $[HNO_3]$ = 1.5 M at 100°C (i.e., midscale on the abscissa), polymer is expected within 100 h.

Finally, the plots of Figs. 23-26 present the interesting linear aspect of this model. It is obvious that plotting Eq. (2) in logarithmic form would give a linear relationship for a fixed acid and temperature. These four figures show the times to form 2% polymer at 25, 50, 70, and 100°C, respectively, for the extreme ranges in $[HNO_3]$ as indicated at the extreme right of each figure. Note also the dashed lines that represent $[HNO_3]$ = 0.2, 0.4, 0.6, and 0.8 M, which is the region often considered to be of greatest interest.

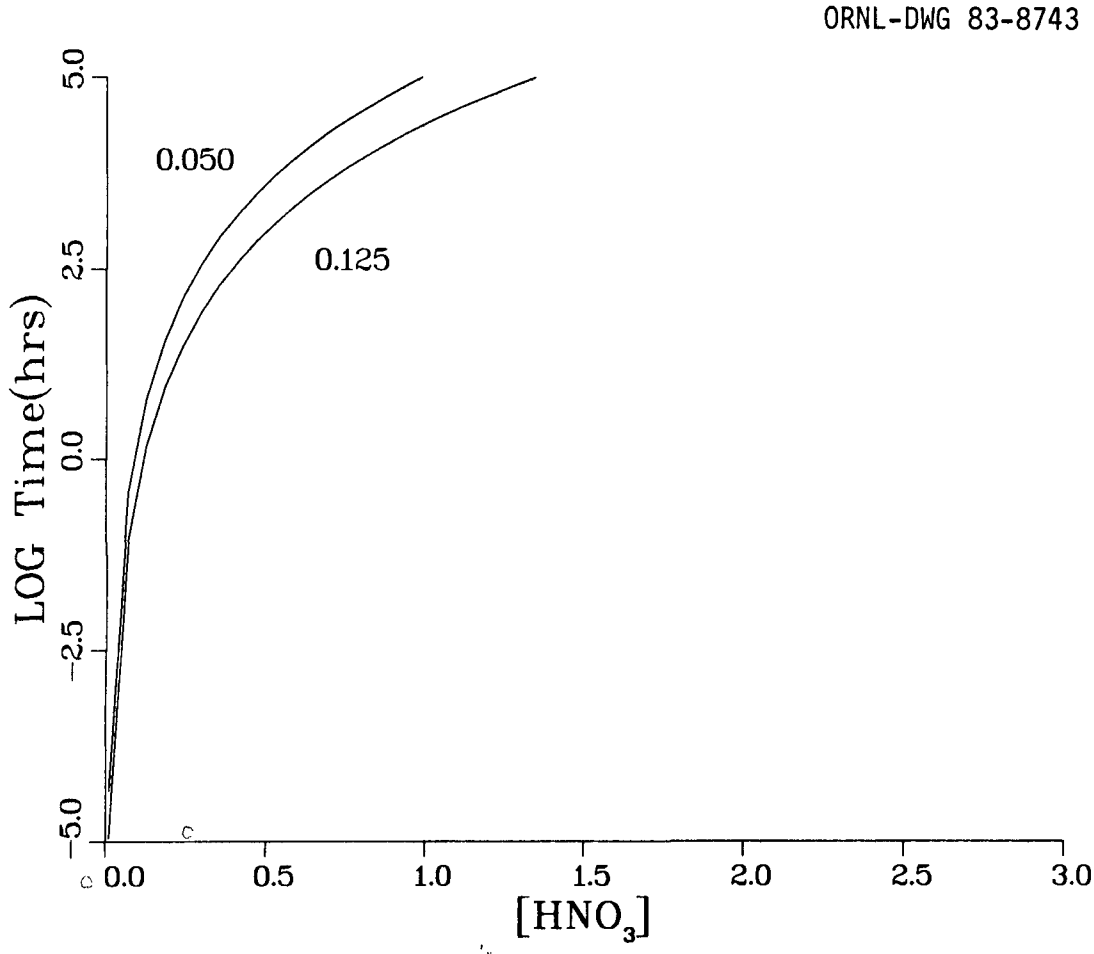

Fig. 19. Extrapolation of the model of Eq. (2) to more extreme acidities at 25°C for 0.05 and 0.125 M [Pu_T], as indicated.

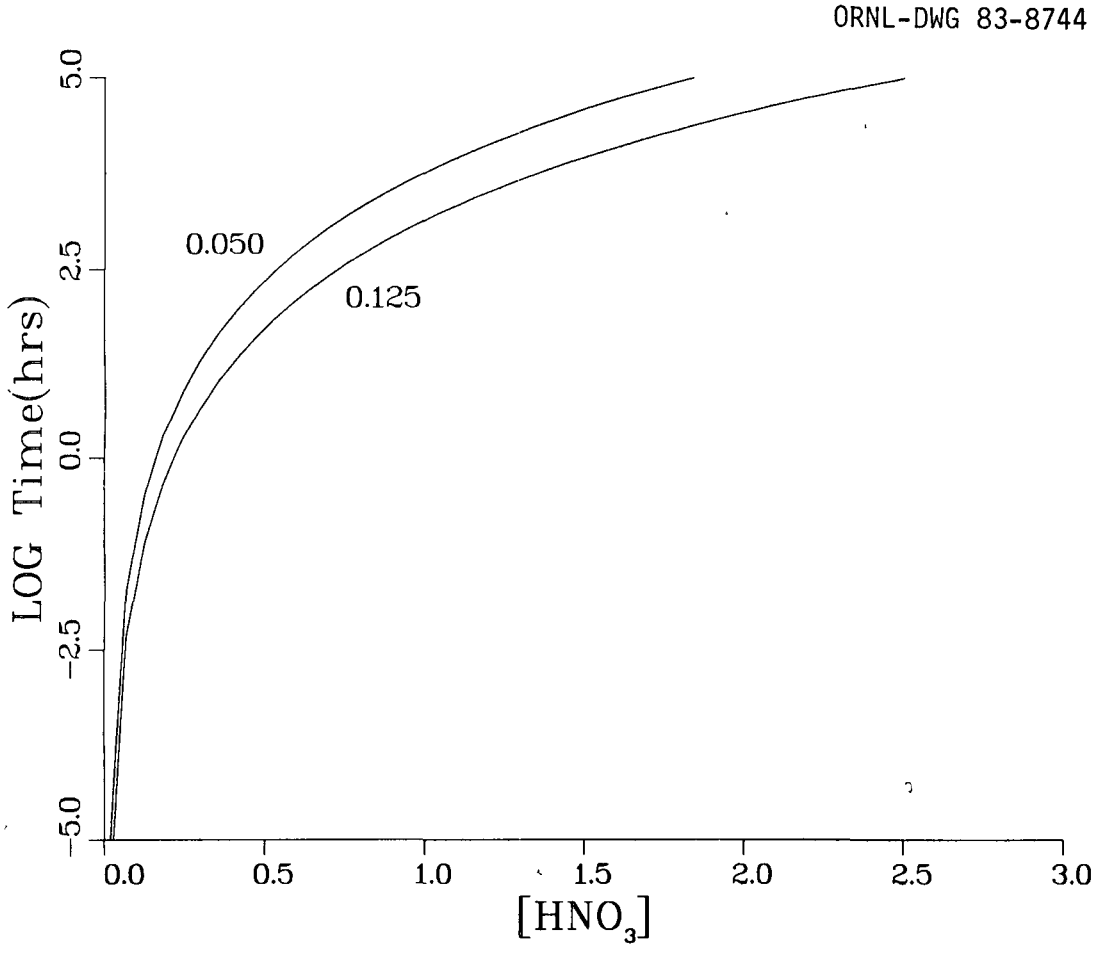

Fig. 20. Extrapolation of the model of Eq. (2) to more extreme acidities at 50°C for 0.05 and 0.125 M $[Pu_T]$, as indicated.

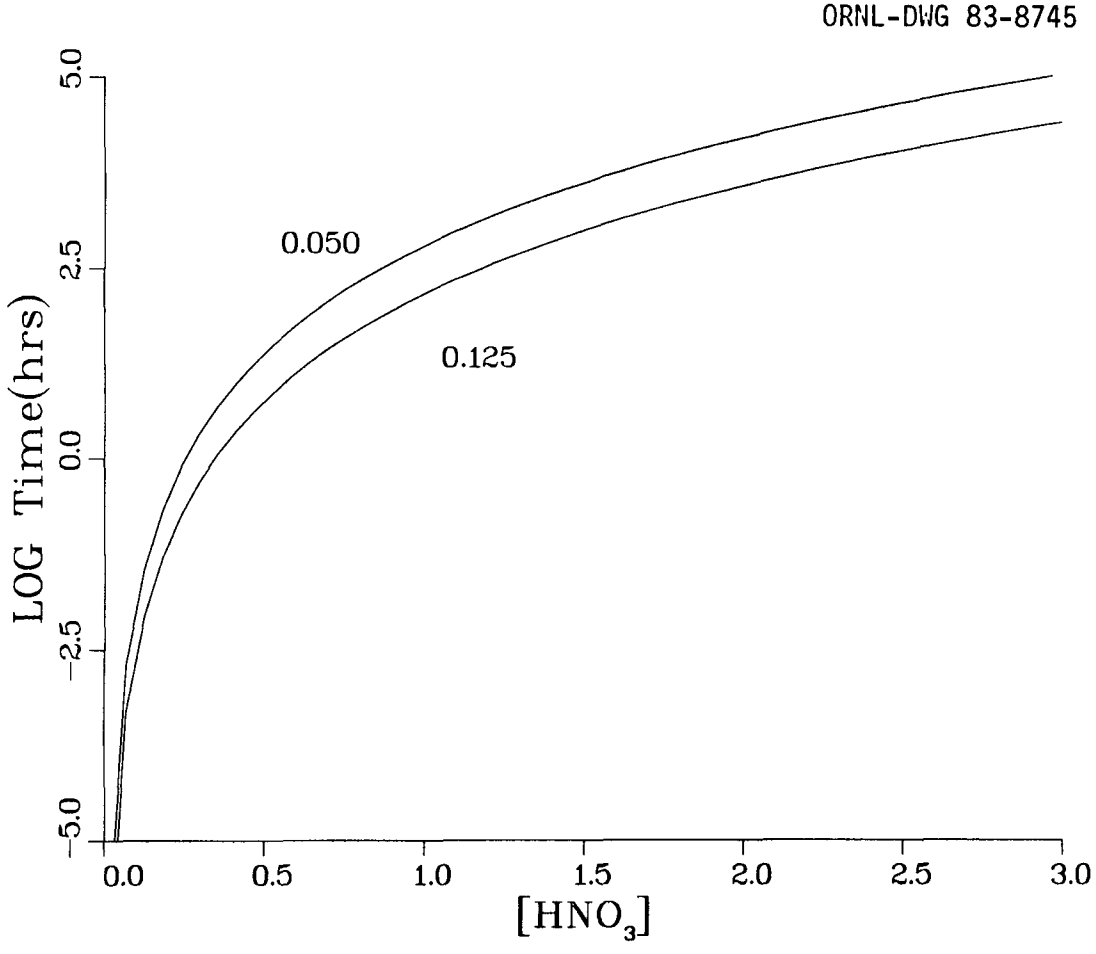

Fig. 21. Extrapolation of the model of Eq. (2) to more extreme acidities at 70°C for 0.05 and 0.125 M $[Pu_T]$, as indicated.

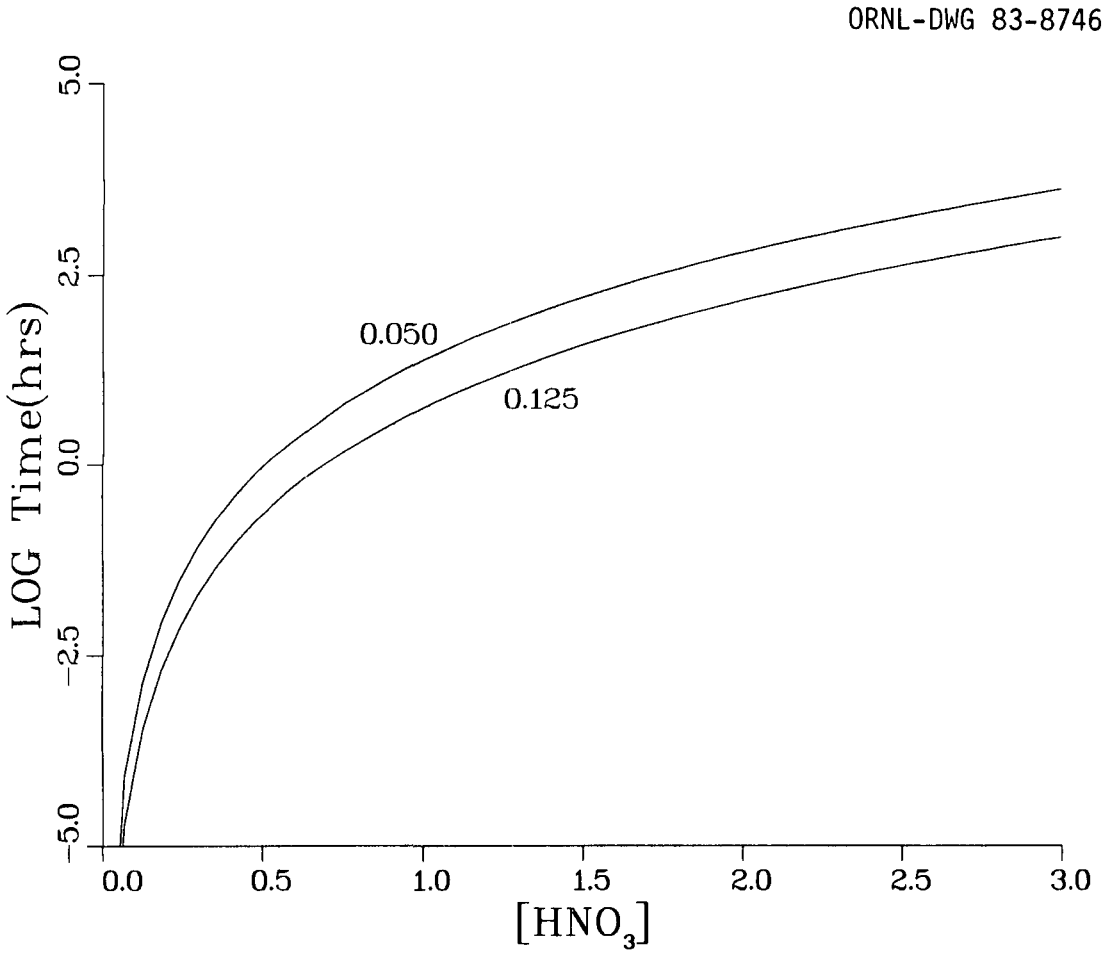

Fig. 22. Extrapolation of the model of Eq. (2) to more extreme acidities at 100°C for 0.05 and 0.125 M $[Pu_T]$, as indicated.

ORNL-DWG 83-8747

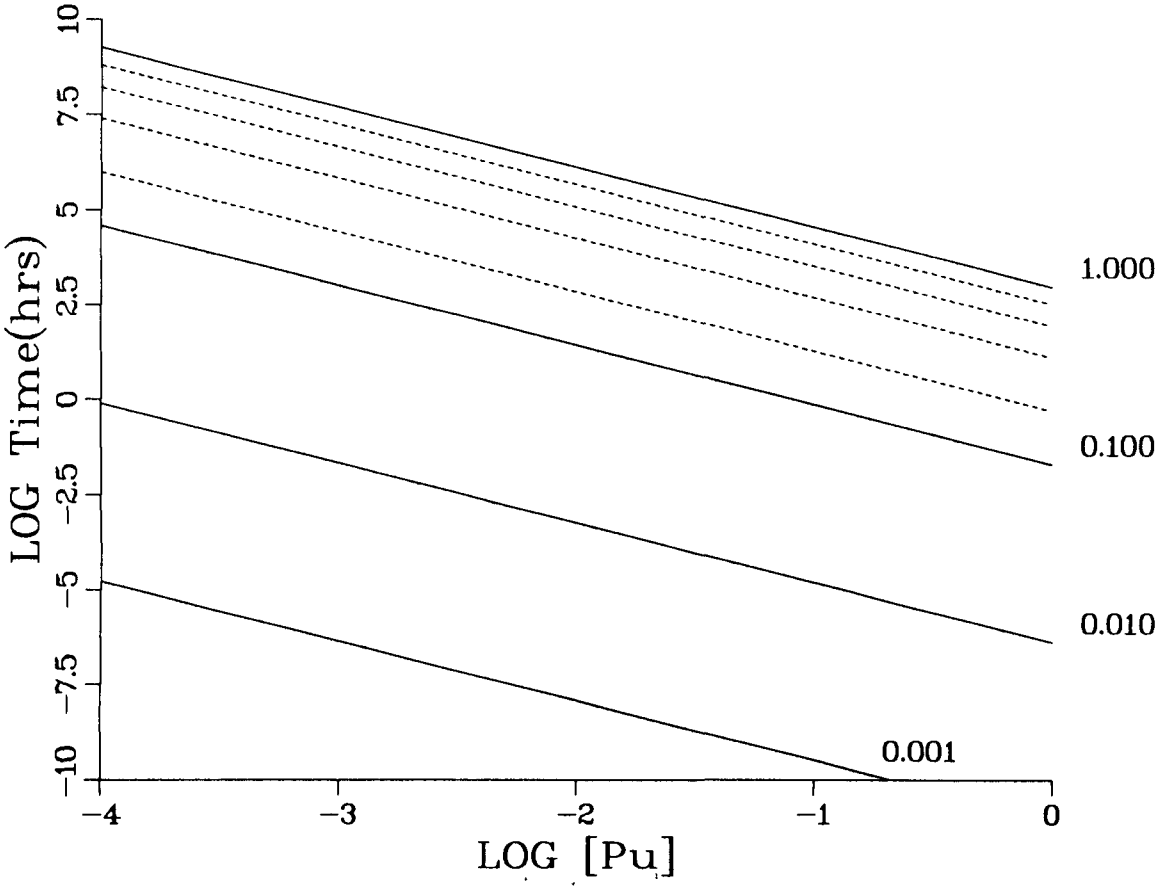

Fig. 23. Plot of log(time) vs log[Pu_T] for the function given in Eq. (2), at 25°C. Slopes are -1.6, the value of the "a" parameter. Solid lines show relationships for 0.001, 0.01, 0.1, and 1.0 M HNO_3, while dashed lines give further subdivision: 0.2, 0.4, 0.6, 0.8 of region between 0.1 and 1.0 M HNO_3.

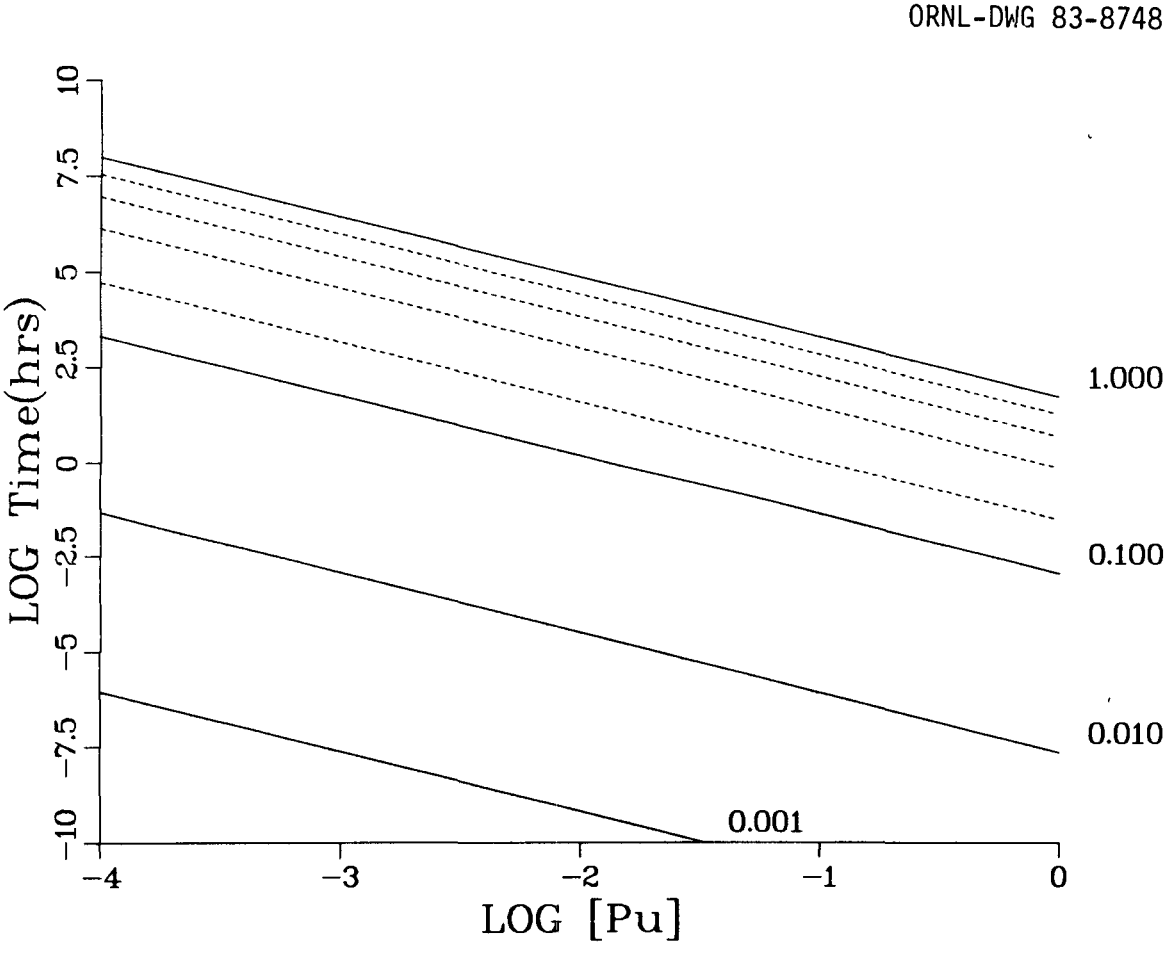

Fig. 24. Plot of log(time) vs log[Pu_T] for the function given in Eq. (2), at 50°C. Slopes are -1.6, the value of the "a" parameter. Solid lines show relationships for 0.001, 0.01, 0.1, and 1.0 M HNO_3, while dashed lines give further subdivision: 0.2, 0.4, 0.6, 0.8 of region between 0.1 and 1.0 M HNO_3.

ORNL-DWG 83-8749

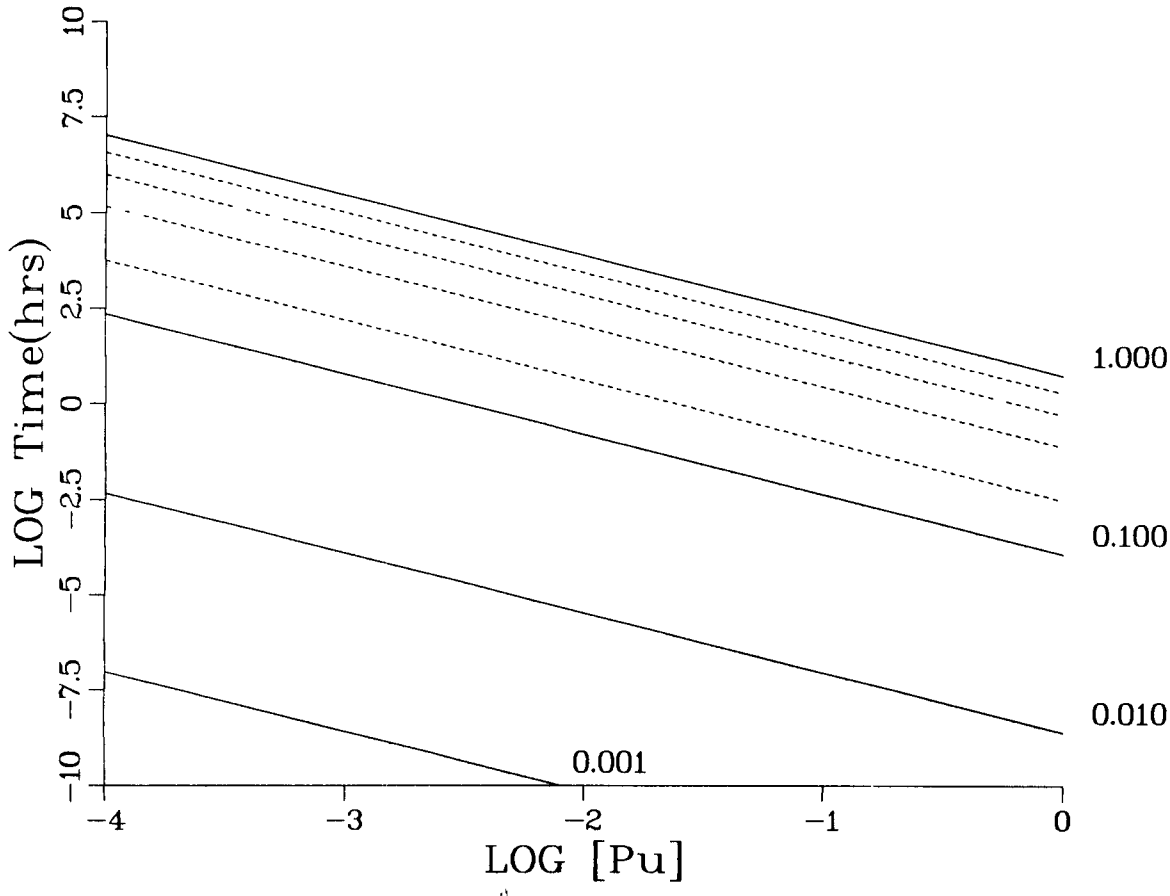

Fig. 25. Plot of log(time) vs log[Pu_T] for the function given in Eq. (2), at 70°C. Slopes are -1.6, the value of the "a" parameter. Solid lines show relationships for 0.001, 0.01, 0.1, and 1.0 M HNO_3, while dashed lines give further subdivision: 0.2, 0.4, 0.6, 0.8 of region between 0.1 and 1.0 M HNO_3.

ORNL-DWG 83-8750

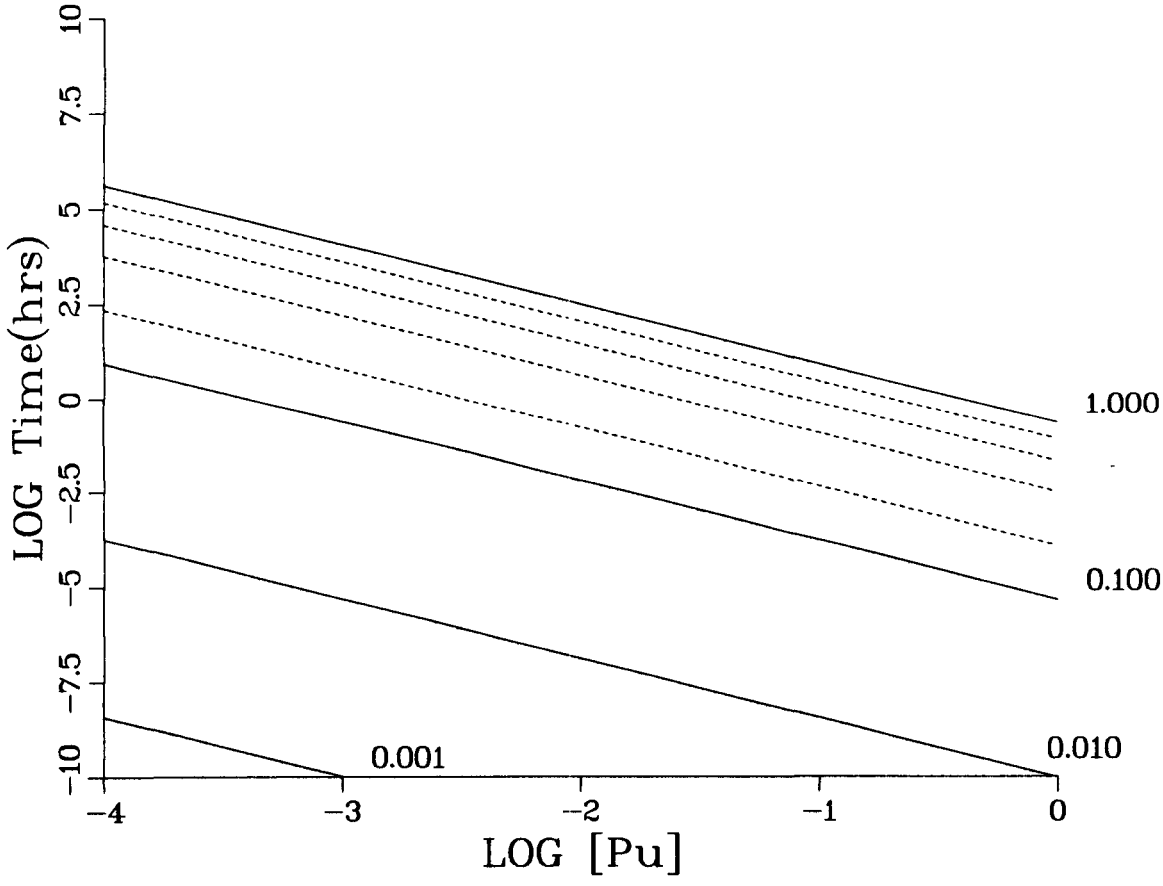

Fig. 26. Plot of log(time) vs log[Pu_T] for the function given in Eq. (2), at 100°C. Slopes are -1.6, the value of the "a" parameter. Solid lines show relationships for 0.001, 0.01, 0.1, and 1.0 M HNO_3, while dashed lines give further subdivision: 0.2, 0.4, 0.6, 0.8 of region between 0.1 and 1.0 M HNO_3.

3.4 EFFECT OF NITRATE ON POLYMER FORMATION RATE

As a final consideration, the effect of excess nitrate ion (added as the salt, $NaNO_3$) was briefly examined. It had been previously shown[1,2] that NO_3^- at concentrations up to 1.0 M and temperatures up to 50°C caused a shift of the disproportionation equilibrium, Eq. (1), to the left by causing an increase in the concentration of the $[Pu(NO_3)]^{3+}$ complex. The associated decrease in the real acid concentration [note the acid dependency of Eq. (1)] could be determined by the change in the concentrations of the individual plutonium ions, and this change in acid concentration was consistent with the observed increase in polymer formation rates.

A few more experiments were performed under a wider range of conditions to establish the general validity of the above observation. At temperatures ≤50°C (the same range examined previously), the added nitrate ion yielded the previously observed results; but at 70°C, the added nitrate ion decreased and/or eliminated polymer formation, suggesting that the role of the NO_3^- ion is extremely complex.

It should be noted that previous references[11] have attributed the enhanced stability of nitrate complexes at high temperatures to a greater relative weakening of the forces of attraction between solvating water molecules and Pu^{4+}, and we believe that this same phenomenon could account for the apparently anomalous NO_3^- effect that we have seen on the polymer formation reaction at 70°C.

Time did not permit a complete examination of the anomaly even though it could offer a means of preventing polymer formation at conditions that would otherwise be conducive to polymerization. Further clarification of the NO_3^- effect on polymer formation is clearly warranted.

3.5 LIMITATIONS AND OTHER CONSIDERATIONS

Although all of the figures (10 through 25) can be computed from the function given in Eq. (2), the large variety is useful in giving a practical viewpoint about Pu(IV) polymer formation. The model is correct in every aspect that we can examine, with one exception — it does not correctly predict that typical Pu(IV) stock solutions, with 0.3 M Pu(IV)

at 1.0 M HNO_3, are stable at 25°C. However, it should be used with caution since other conditions may alter the polymer kinetics. Most significant among these conditions is reflux, which is too complex to model.[3] The presence of UO_2^{2+}, on the other hand, should not alter the model predictions by more than a factor of 2; and since any alteration would be in the direction of reducing the rate of polymerization,[1,2] the model would simply give a conservative representation of the polymer problem. Nitrate ion, in excess of that associated with the $UO_2(NO_3)_2$ stoichiometry, is the least studied of these other influences and, for reasons stated earlier, requires more consideration. The effect of high nitrate concentrations on solutions that are taken to dryness would be particularly significant. By far, the most severe limitation to the use of this model is recognized to be associated with conditions where low-acid diluents are mixed with the Pu(IV) solution at temperatures ≥70°C, either through reflux or other means. Under such conditions, very rapid and irreversible polymer formation is almost a certainty.[3]

4. CONCLUSIONS

The polymer formation reaction can be described either in formal terms or as a simplified model. Regardless of the approach, it is possible to predict the kinetic rates and times before the appearance of polymer based solely on the knowledge of T, $[HNO_3]$ and $[Pu_T]$. The primary goal achieved in this study is the development of a simple model that fits the measured data very well and has a form that is physically realistic. Although the adjustable parameters do not fit the measured orders of the reaction (and are not expected to fit them under the approximations used here), they are surprisingly close to the fundamentally determined parameters. The influence of NO_3^- on polymer formation at temperatures greater than 50°C needs more consideration.

5. ACKNOWLEDGMENTS

The authors with to express their gratitude to M. H. Lietzke, Chemistry Division, for his generous advice and guidance in the application of the least squares computer program. Thanks are also extended to M. E. Whatley, Fuel Recycle Division, for his many helpful suggestions.

6. REFERENCES

1. L. M. Toth, H. A. Friedman, and M. M. Osborne, The Polymerization of Pu(IV) in Aqueous Nitric Acid Solutions, ORNL/TM-7180, October 1980.

2. L. M. Toth, H. A. Friedman, and M. M. Osborne, J. Inorg. Nucl. Chem. 43(11), 2929 (1981).

3. L. M. Toth and M. M. Osborne, The Effect of Reflux on the Rate of Pu(IV) Hydrous Polymer Formation, ORNL/TM-8240, June 1982.

4. Display Integrated Software Systems and Plotting LAnguage, Integrated Software Systems Corp., San Diego, Calif., 1975.

5. C. L. Lawson, "Brief Users' Guide for C^1 Surface Interpolation Subroutines," Sect. 366, Computing Memorandum No. 430, Jet Propulsion Laboratory, California Institute of Technology, Pasadena, Calif., Aug. 25, 1977.

6. J. M. Cleveland, The Chemistry of Plutonium, Gordon and Breach Science Publishers, New York, 1970, p. 24.

7. G. P. Tkhorzhnitskii, V. I. Medvedovskii, and G. F. Egorov, Radiokhimiya 23, 376 (1981).

8. M. H. Lietzke, A Generalized Least Squares Program for the IBM 7090 Computer, ORNL-3259, March 1962.

9. See, for example: E. A. Moelwyn-Hughes, Proc. Roy. Soc. A164, 295 (1938); J. C. Kendrew and E. A. Moelwyn-Hughes, Proc. Roy. Soc. A176, 352 (1940); P. Johnson and E. A. Moelwyn-Hughes, Proc. Roy. Soc. A175, 118 (1940).

10. M. E. Whatley, Oak Ridge National Laboratory, private communication.

11. J. M. Cleveland, The Chemistry of Plutonium, Gordon and Breach Science Publishers, New York, 1970, p. 112.

ORNL/TM-8665
Dist. Category UC-86T
(Applied)

INTERNAL DISTRIBUTION

1. J. M. Begovich
2-3. J. T. Bell
4. D. E. Benker
5. W. D. Bond
6-8. W. D. Burch
9. D. O. Campbell
10. J. L. Collins
11. D. A. Costanzo
12. R. M. Counce
13. D. J. Crouse
14. F. C. Davis
15. R. V. Eberle
16. R. D. Ehrlich
17. M. J. Feldman
18. R. L. Fellows
19. R. W. Glass
20. W. S. Groenier
21. D. C. Hampson
22. A. L. Harkey
23-24. J. R. Hightower
25. E. K. Johnson
26. R. T. Jubin
27. M. V. Keigan
28. H. T. Kerr
29. L. J. King
30. R. E. Leuze
31. B. E. Lewis
32. J. C. Mailen
33. D. D. McCue
34. J. G. Morgan
35. E. L. Nicholson
36. R. E. Norman
37-41. M. M. Osborne
42. E. D. North
43. K. D. Pannell
44. R. L. Philippone
45. R. T. Primm, III
46. D. J. Pruett
47. R. H. Rainey
48. J. H. Shaffer
49. J. H. Stewart, Jr.
50-51. M. G. Stewart
52. J. G. Stradley
53. O. K. Tallent
54-58. L. M. Toth
59. M. E. Whatley
60. S. K. Whatley
61. J. E. Wortman
62. R. G. Wymer
63. O. O. Yarbro
64. H. R. Yook
65. Manson Benedict (consultant)
66. A. Schneider (consultant)
67-68. Laboratory Records
69. Laboratory Records-RC
70. ORNL Patent Section

EXTERNAL DISTRIBUTION

71-72. K. O. Laughon, Jr., Director, Office of Spent Fuel Management and Reprocessing Systems, U.S. Department of Energy, Washington DC 20545
73. F. P. Baranowski, 1110 Dapple Grey Court, Great Falls, VA 22066
74. S. J. Beard, Vice President, Marketing and Uranium Operations, Exxon Nuclear Company, Inc., 600 108th Avenue, N.E., C-00777, Bellevue, WV 98009

75. R. Little, Princeton Plasma Physics Laboratory, James Forrestal Campus, P.O. Box 451, Princeton, NJ 08544
76. J. L. McElroy, Pacific Northwest Laboratories, P.O. Box 999, Richland, WA 99352
77. M. J. Ohanian, Associate Dean for Research, College of Engineering, 300 Weil Hall, University of Florida, Gainsville, FL 32611
78. J. F. Proctor, E. I. duPont de Nemours and Company, Montchanin Building 6600, Wilmington, DE 19898
79. Office of Assistant Manager for Energy Research and Development, DOE-ORO, Oak Ridge, TN 37831

80-124. Given distribution as shown in TIC-4500 under UC-86T, Consolidated Fuel Reprocessing Category.

Missing Page
from
Original Document

Missing Page
from
Original Document

CONTENTS